UNIVERSITY OF CANTERBURY

DOCTORAL THESIS

Artistic Style Characterization of Vincent van Gogh's Brushstrokes

Author:

Tieta PUTRI

Supervisors:

Assoc. Prof. R. MUKUNDAN

Dr. Kourosh NESHATIAN

A thesis submitted in fulfillment of the requirements

for the degree of Doctor of Philosophy

March 15, 2019

Declaration of Authorship

I, Tieta PUTRI, declare that this thesis titled, "Artistic Style Characterization of Vincent van Gogh's Brushstrokes" and the work presented in it are my own. I confirm that:

- This work was done wholly or mainly while in candidature for a research degree at this University.
- Where any part of this thesis has previously been submitted for a degree or any other qualification at this University or any other institution, this has been clearly stated.
- Where I have consulted the published work of others, this is always clearly attributed.
- Where I have quoted from the work of others, the source is always given. With the exception of such quotations, this thesis is entirely my own work.
- I have acknowledged all main sources of help.
- Where the thesis is based on work done by myself jointly with others, I have made clear exactly what was done by others and what I have contributed myself.

Signed: 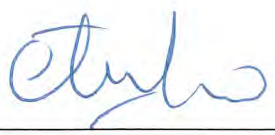

Date: 15 March 2019

"That brain of mine is something more than merely mortal, as time will show."

Ada Lovelace

"We can know only that we know nothing. And that is the highest degree of human wisdom."

Leo Tolstoy (War and Peace)

UNIVERSITY OF CANTERBURY

Abstract

College of Engineering

Department of Computer Science and Software Engineering

Doctor of Philosophy

Artistic Style Characterization of Vincent van Gogh's Brushstrokes

by Tieta PUTRI

Automatic style characterization is the process of measuring, extracting, and analysing different formal elements. Brushstroke technique, in conjunction with other formal elements such as colour and texture, play a vital role in defining an artistic style. This thesis explores the stroke-based style analysis of the paintings of Vincent van Gogh, who is well-known for his use of wide and repetitive brushstrokes. Novel brushstroke extraction techniques are used to segment and analyse Van Gogh's brushstrokes. The extracted features can then be compiled into a feature set which represents the quantified brushstrokes' properties and tested using several classification-based tests. The most contributing factor for detecting visible brushstroke is the brushstroke's texture, due to the fact that the texture-based segmentation methods give more satisfactory results in extracting visible brushstrokes with their average classification accuracy and F-measure being 98.30% and 0.973 respectively.

Acknowledgements

First and foremost, I would like to thank my supervisor, Associate Professor Ramakrishnan Mukundan for his unending support and encouragement during my study. Dr. Mukundan had always motivated me to be my better self and reminded me that I will always be all right. I am also thankful for my associate supervisor, Dr. Kourosh Neshatian, for his suggestions in the machine learning aspects of this project.

I thank my friends and family who have constantly remind me that I am loved and I matter. I thank those who always been there for me, especially when things turn to be not as cheery as expected: Alex da Silva, Shah Munir, Cybele Freitas, Wendy and Mark Kilpatrick, Philip and Christina Vesty, Frances Ogier, Yalini Sundralingam, Fr. Michael-Therese Scheerger, Fr. Clement Covacho, and Ivonne Margi Immanuella.

I offer special thanks to my mother, who loves me no matter what and inspires me with her strength and motivation to never give up on life.

And finally, last but by no means least, for my beloved other half, Julian Vesty. He made me laugh, wiped my tears, hugged me tight, seen me fail, watched me succeed, and most importantly, kept me strong.

"Love alters not with his brief hours and weeks,
But bears it out ev'n to the edge of doom."
- *Sonnet 116 (William Shakespeare)*

Contents

List of Figures

List of Tables

List of Abbreviations

CA	**C**uno **A**miet
CCV	**C**olour **C**oherence **V**ector
CFS	**C**orrelation-based **F**eature **S**ubset
CNN	**C**onvolutional **N**eural **N**etwork
DBSCAN	**D**ensity-**B**ased **S**patial **C**lustering of **A**pplications with **N**oise
ESH	**E**dge **S**ize **H**istogram
FN	**F**alse **N**egative
FP	**F**alse **P**ositive
GLCM	**G**ray **L**evel **C**o-occurrence **M**atrix
HoG	**H**istogram **o**f **G**radient
ID3	**I**terative **D**ichotomizer 3
IQR	**I**nter-**Q**uartile **R**ange
LBP	**L**ocal **B**inary **P**attern
MATLAB	**MAT**rices **LAB**oratory
MDL	**M**inimum **D**escription **L**ength
MHN	**M**aximum **H**omogeneity **N**eighbour
MLP	**M**ulti **L**ayer **P**erceptron
NPR	**N**on-**P**hotorealistic **R**endering
NSC	**N**eutrosophic **S**et **C**lustering
PCA	**P**rincipal **C**omponent **A**nalysis
PR	**P**hotorealistic **R**endering
POET	**P**revailing **O**rientation **E**xtraction **T**echnique
RGB	**R**ed **G**reen **B**lue

SBR	**S**troke **B**ased **R**endering
SNN	**S**ymmetric **N**earest **N**eighbour
SAR	**S**ynthetic **A**perture **R**adar
SOM	**S**elf **O**rganizing **M**ap
SIFT	**S**cale **I**nvariant **F**eature **T**ransform
SVM	**S**upport **V**ector **M**achine
TN	**T**rue **N**egative
TP	**T**rue **P**ositive
WEKA	**W**aikato **E**nvironment for **K**nowledge **A**nalysis

Julian, this is for you darling.

Chapter 1

Introduction

1.1 Overview

In Art History, formal analysis of painting aims to explain and correlate different elements of artworks to their content. The elements that are observed in formal analysis are called *the formal elements*, and the repeating occurrence of a particular element throughout a collection of work is considered as a *style*. Style plays an important role in defining a painting's aesthetic value (Dutton, 2009). According to Dutton (2009), the influence of a painter or an art movement is determined by the distinguishable, recurring, and consistent style that is present in the artworks. For instance, the art movement of Impressionism is well-known for its vivid colour, thick application of painting, and life subject matter. The combination of those three elements formed the Impressionist style which was popular in the late nineteenth century France.

To be able to correctly identify a style of an artist or era, the observer must have a great understanding of formal analysis and an eye for details which are able to identify recurring characteristics of many paintings. The *connoisseurs* are observers who are considered as the best judge due to their deep knowledge in a particular arts subject. Today, the art of connoisseurship

continues to thrive, despite its immense reliance on self-proclaimed expertise that can potentially cause disputes.

To meet the challenging requirements of style characterization, researchers in computer vision have been developing novel algorithms to correctly identify elements of style. Since style is distinguishable, recurring, and consistent (Dutton, 2009), it can be formulated as a pattern recognition problem (Kroner and Lattner, 1998; Li et al., 2012; Johnson et al., 2008; Lee and Cha, 2016). It has many applications in archiving and cataloguing artworks (Johnson et al., 2008; Jiang et al., 2006; Icoglu, Gunsel, and Sariel, 2004), building a content-based image retrieval system (Putri and Arymurthy, 2010), distinguishing contemporaries (Li et al., 2012), and helping art education in museums and galleries. One of the many advantages of automatic style characterization is that it can serve as a tool to complement manual inspection and to discover relationships between artworks (Li et al., 2012).

a

b

FIGURE 1.1: Two paintings by the same artist, Vincent van Gogh, from different periods: (a) *Self-portrait with Straw Hat* (1887, Paris) and (b) *Wheatfield with Crows* (1890, St. Rémy). Van Gogh's works between 1885-1890 had built an *ouvre*, which is a collection that reflects his personal vision. Although these two paintings came from his two different art periods, they contain elements which had made them descriptive to Van Gogh's *ouvre*, which are the optimal use of colour, perspective and brushstroke (Van Uitert, 1981).

a b

FIGURE 1.2: Two paintings by different artists from different art movements: (a) *Luncheon at the Boating Party* (1881) by Pierre-Auguste Renoir, and (b) *Sunflowers (Fourth Version)* (1888) by Vincent van Gogh.

Automatic style characterization in the process of measuring, extracting, and analysing different formal elements, such as brushstroke technique, colour, and texture. According to Zang, Huang, and Li (2013), brushstroke technique, in conjunction with other elements such as colour and texture, play a vital role in defining an artistic style. For instance, the Pointillist style is defined as consisting of small, elliptical and repeated brushstrokes that are put together in such way that it will form the object when a viewer looks at it from a certain distance. This argument has motivated considerable research into mathematical and computational brushstroke analysis.

This thesis explores the stroke-based style analysis of the paintings of Vincent van Gogh, a post-impressionist who is best known for his use of wide and repetitive brushstrokes, a technique known as *impasto*. His works are of interest in this thesis because of the many contemporaries with similar style as him. In addition, we also want to examine the features of his brushstrokes compared to other painters, including those of his contemporaries.

We will see how novel brushstroke extraction techniques are used to segment and analyse Van Gogh's brushstrokes. The extracted features can then be compiled into a feature set which serves as the quantified brushstrokes' properties and tested using several classification-based tests.

1.2 Research Objectives

The general objectives of this thesis are to:

1. Identify important brushstroke features for characterizing style.
2. Develop a characterization framework that can distinguish works of art based on the brushstroke features.

The specific objectives of this thesis are to:

1. Develop novel methods to identify Van Gogh's visible brushstrokes.
2. Determine characteristics of Van Gogh's brushstrokes by identifying the brushstrokes' shape and texture.
3. Compare, classify, and analyse the style of Van Gogh with other painters.

1.3 Research Questions

The research questions that are going to be answered in this thesis are:

1. How can visible brushstrokes be segmented from Van Gogh's painting?
2. How should we determine the style features from Van Gogh's brushstrokes?

3. Can the brushstroke features be used to distinguish Van Gogh's works from other painters'?

1.4 Research Relevance and Motivation

This research is a cross-disciplinary research between arts and computer science. It addresses an element of art historiography, which is style characterization, by incorporating pattern recognition algorithm as a new observational tool (Kroner and Lattner, 1998; Li et al., 2012; Johnson et al., 2008; Lee and Cha, 2016). One of the many advantages of automatic style characterization is to discover supporting evidence for settling scholarly disputes in classifying artworks (Coburn et al., 2010; Johnson et al., 2008; Jiang et al., 2006; Icoglu, Gunsel, and Sariel, 2004). Many are trying to accomplish the task by identifying the 4W1H of art creation: *what* the object of the art is, *who* created the art, *where* the art was created, *when* the period of the art was, and *how* the art was made. Even art experts struggle to identify and classify artworks correctly and often disagree with each other's classification systems. This research will hopefully provide assistance for art experts by providing additional useful information from the brushstroke features of an artwork that cannot be identified visually. In addition, it can also serve as a tool to discover relationship between artworks (Li et al., 2012).

Similar to the classification task, cataloguing and retrieving artworks based on their content can be achieved by taking the artwork's properties as metadata that serves as searching attributes. Correctly assigning these metadata is important for getting the proper precision and recall. In order to achieve that, a semantic analysis of the artwork can be performed by separating the style from the content (Gatys, Ecker, and Bethge, 2015) and assessing its

FIGURE 1.3: The example of pointillist-NPR (middle)with the photograph of Eiffel tower as the target image (left) and its comparison to a pointillist painting of Eiffel tower (right) (Putri, 2012).

content. The work of Gatys, Ecker, and Bethge (2015) will be elaborated further in Subchapter 2.3.

Automatic style characterization is also important in the field of non-photorealistic rendering (NPR). As the aim of NPR is to produce images with artistic appearance, the style extracted by the algorithm proposed in this research provides a certain level of abstraction to the target image. In NPR, the style features are mapped to the photographic target image as a series of pixel-placement instructions. This process is similar to the conventional painting activity, where artists identify the style of great masters by observation and apply it as a set of rules to visualize their object.

Many automatic style characterization done by researchers emphasized on whole painting characterization (Gatys, Ecker, and Bethge, 2015; Chu and Wu, 2018; Hughes, Graham, and Rockmore, 2010; Sener, Samet, and Sahin, 2012; Agarwal et al., 2015). Their works examined the artworks as a unity, that is, as a whole structure constructed by their formal elements. By doing so, style was extracted as a concrete element which can be transferred into

another object matter. Contrariwise, it can also appear as an intangible set of rules which cannot be conformed to the traditional formal elements of painting.

In contrast to the previous approach, automatic style characterization by identifying the artwork's formal elements is seen as a more definite procedure. It addresses the classical method of art historiography by incorporating automation of formal analysis of the artwork's elements. Many works in this approach is done by observing elements such as colour (Lee and Cha, 2016), light (Icoglu, Gunsel, and Sariel, 2004; Kroner and Lattner, 1998), texture (Taylor, Micolich, and Jonas, 1999), composition (Lee, Olsen, and Gooch, 2006), and brushstrokes (Jiang et al., 2006; Sheng and Jiang, 2013; Li et al., 2012; Putri and Arymurthy, 2010; Berezhnoy, Postma, and Van Den Herik, 2009; Johnson et al., 2008). More research has gone towards brushstroke-based artistic style characterization due to the fact that it is considered as the most important element of a visual artwork (Urmson, 1989; Dutton, 2009). Brushstrokes provide information that is not only related to the subject matter and how the painter wanted it to be perceived by the viewers, but also related to the painter and his/her artistic background.

The most important challenge in the stroke-based artistic style is to correctly segment the brushstroke regions so that accurate features can be obtained from them. The regions can be acquired using various region extraction methods, such as statistical methods (Mori and Mori, 2012), set-based extraction (Pal, 1992), gradient-based thresholding (Yan, Sang, and Zhang, 2003) and connected component labelling (Samet, 1981; Sheng and Jiang, 2013). This research identifies and analyses features obtained from brushstrokes of Van Gogh's paintings. The brushstrokes in this research is extracted by the iterative extraction method, texture boundary detection method, Gabor filter based segmentation method, and neutrosophy-based

segmentation method. The novelty of this thesis is shown in the implementation of those four segmentation method. It is also shown in the demonstration of the significance of semantically-relevant brushstrokes feature,such as texture, and shape, to the style of a painting.

1.5 Research Contributions

The contributions of this research are:

1. Iterative extraction method using homogeneity measure and maximum homogeneity neighbours (MHN) filter. (Putri and Mukundan, 2015) This method is a faster alternative to the classic connected component labelling that is based on homogeneity between neighbours. It will be elaborated further in Subchapter 3.5.1.

2. Visible brushstroke extraction method with neutrosophy-based image segmentation and circular filter. This method converted the paintings' pixels from the image processing domain in CIELAB colour space to neutrosophic domain (Smarandache, 1999). The neutrosophic domain is commonly used by researchers to remove noise in medical images. The motivation for using it in this research is because of the nature of visible brushstrokes, which have concealed brushstrokes surrounding them. The concealed brushstrokes can neither be classified as a prominent brush stroke nor as a non-brushstroke. The image is preprocessed using circular filter to magnify the brushstrokes' elliptical shape, then converted to neutrosophic domain. It will be elaborated further in Subchapter 3.5.2.

3. Texture-based visible brushstroke segmentation using texture boundary detection and Gabor filter (Putri, Mukundan, and Neshatian,

2017). These two segmentation methods used texture-based algorithms for segmenting visible brushstrokes in Van Gogh's painting. Its development was motivated by an observation that suggested that a brushstroke region has its own texture due to the brush movement and paint spread. It will be elaborated further in Subchapter 3.5.3 and 3.5.4.

4. Classification of Van Gogh's painting from his Impressionist predecessors and his contemporary, Cuno Amiet (Putri, Mukundan, and Neshatian, 2017). From the features that we obtained from segmented brushstrokes, we classified Van Gogh's paintings from other painters with similar brushstroke properties. The classification result showed that the features we obtained from brushstroke regions represents Van Gogh's painting style very well.

1.6 List of Publications

During the construction of this thesis, we have published these articles below:

1. Putri, T., & Mukundan, R. (2016, March). Iterative Brush Path Extraction Algorithm for Aiding Flock Brush Simulation of Stroke-Based Painterly Rendering. In *International Conference on Evolutionary and Biologically Inspired Music and Art* (pp. 152-162). Springer, Cham. `https://doi.org/10.1007/978-3-319-31008-4_11`.

2. Putri, T., Mukundan, R., & Neshatian, K. (2017). Artistic Style Characterization of Vincent Van Gogh s Paintings using Extracted Features from Visible Brush Strokes. In ICPRAM (pp. 378-385). `https://doi.org/10.5220/0006188303780385`.

3. Putri, T., Mukundan, R., & Neshatian, K. (2017, December). Artistic style characterization and brush stroke modelling for non-photorealistic rendering. In 2017 International Conference on Image and Vision Computing New Zealand (IVCNZ). IEEE. https://doi.org/10.1109/ivcnz.2017.8402475.

4. Putri, T., Mukundan, R., & Neshatian, K. (2018, December). Neutrosophic Extraction of Vincent van Gogh's Visible Brush Strokes. In 2018 International Conference on Image and Vision Computing New Zealand (IVCNZ). https://doi.org/10.1109/ivcnz.2018.8634702.

1.7 Research Scope and Limitation

The scope of this thesis falls within the stroke-based approach for capturing painting style. The main goal is to characterize the painting style of Vincent van Gogh by extracting representative features from his brushstrokes using novel image segmentation algorithm. Van Gogh's works are chosen due to his distinguishable visible brushstroke characteristics which are bold, wide, repetitive and have the ability to depict objects with a certain level of abstraction.

The brushstroke extraction aims to extract the strokes that are clearly visible to the viewers eyes. Concealed strokes, the ones that are not visible enough due to their size or physical structure, are not considered in the extraction. This visible brushstroke extraction process decreases the ability of the characterization of paintings with blended strokes, such as paintings in the realist style. However, characterization can still be done by extracting additional features that are related to the painting's subject matter and/or composition.

Chapter 2

Artistic Style Characterization

2.1 Introduction

Every artwork can be seen as a structure of two building block, which are the style, and the content, which is also known as the subject matter (Gatys, Ecker, and Bethge, 2015). Style is a series of distinguishable and recurring characteristics which allows artistic works to be categorized into groups (Dutton, 2009). A single content can be visualized in different styles, depending on the artist's perception or the message the artist wants to convey.

The task of artistic style characterization is the process of identifying and extracting the style elements of artworks and group them as a series of features. It has been of an interest of art historians since the publication of Giorgio Vasari's *The Lives of The Most Eminent Italian Architects, Painters, and Sculptors* (1568). Vasari's work contains the biographies of Italian artists along with the descriptions of their works' characteristics. It has been recognized as the first important book in art history and became the intellectual bedrock of subsequent art historiography.

This chapter describes the manual and automatic characterization of paintings and their applications.

2.2 Manual Characterization

2.2.1 Formal Analysis of Paintings

Art historians have done extensive technical analysis to correctly describe, discuss, and classify paintings. Each of them has a different way of analysing a certain work of art. Similar characteristics that are present in different paintings may potentially cause disputes between art historians in classifying paintings. According to Lombardi, Cha, and Tappert (2004), descriptive properties for painting analysis can be divided into three categories: physical, subjective, and formal. The physical properties are related to the painting's contextual aspect, such as medium, creator, and date of work. In contrast, the subjective properties cover the aspects that describe the content of the artwork, such as its title; and type of subject matter, such as people, objects, or landscapes. Different from the physical and subjective properties, the formal property covers the question on *how* an artist paints the subject matter.

Formal analysis identifies different elements of art which are considered as the building blocks to the work. Those elements that are commonly employed for a formal analysis are (Lombardi, Cha, and Tappert, 2004): light, line, colour, and texture. Light renders high or low regions of contrast and illusionist space by depth representation. Lines serve as the building blocks of the object matter's shapes. They also allow composition and spatial organization and even texture of the painting. Artists generate lines by forming brushstrokes on the medium. Some aspects that are related to brushstrokes include thickness, length, orientation, and shape. Several line placement techniques such as cross-hatching, overlapping, and shading are also taken into account in the observation. Lines can also be implicitly defined as a

boundary between to regions. Texture represents the coarseness or smoothness of the painting's surface. There are two different kinds of texture: the perceived, which is generated by the artist to render the texture of the subject matter, and actual texture of the paint on the medium. Colours are observed in terms of three aspects: hue, which defines the tint of the colour; saturation, which represents the intensity of the colour; and value, which is the brightness of the colour.

2.2.2 Connoisseurship

Connoisseurs are regarded as the best judges in a particular field and their judgements are highly respected. They have a great knowledge in the subjects that are related to taste and aesthetics, such as the fine arts and culinary arts. The purpose of connoisseurship is to correctly identify genuine works from their copies by the artist's contemporaries and forgers; and to sort them chronologically. It is considered as an important skill to have, especially when the works are lacking in documented evidence of provenance (Carrier, 2003).

Things that are identified by connoisseurs are: provenance, dating, attribution to individual masters, and authenticity. Other than those, connoisseurs also identify the artwork's size, condition, medium, technique, quality, and formal characteristics (Kleinbauer and Slavens, 1982). The term *connoisseur* was first introduced by a London-based portrait painter Jonathan Richardson the Elder in 1719. It was the time when connoisseurship was popular amongst art historians in Europe. due to the growth of the number of art transactions across the continent. This fact has motivated some scholars to further investigate the techniques of connoisseurship. One of those scholars is Carl Friedrich von Rumohr. In his published work *Italianische*

Forschung, he outlined the history of Italian paintings and sculptures. *Italianische Forschung* described the attribution of artworks based on available evidences and the study of philology. It has also empirically distinguished original artwork from its copy. Because of these two significant contributions, the work of Von Rumohr is deemed to be an important contribution in the historiography of art.

Giovanni Morelli (pseudonym: Ivan Lermolieff-Schwarze) was the first person to formulate and rationalize the task of connoisseurship in the late nineteenth century. Being an expert in anatomy, Morelli had successfully authenticated Renaissance portraits by analysing anatomical details of the subject matter. Morelli's methodology and findings were deemed to be very significant, given the current nature of connoisseurship at that time which relied highly on the opinions of experts, most of them self-proclaimed (Kleinbauer and Slavens, 1982).

Morelli's authentication method has become popular ever since. A particularly noteworthy follower of the method was Bernard Berenson. Berenson enhanced Morelli's method by incorporating written sources for his identification rather than solely relying on his own observation. Although he was known as "The Connoisseur of Connoisseurs", he was also involved in many authentication disputes (Charney, 2015). One of those disputes was the Duveen case, when Berenson was commissioned to authenticate a sixteenth century painting called *The Allendale Nativity*.

In 1937, the art dealer Joseph Duveen promised Berenson a generous payment if he could prove that the painting was by Giorgione (Sutton, 1987). The reason was so that he could sell it to Samuel Kress, a wealthy philanthropist and art collector. Duveen wanted the painting to be Giorgione's as Giorgione's works are highly valuable, given that the painter died of plague at a young age of thirty-two after producing just five surviving paintings.

FIGURE 2.1: *The Allendale Nativity* by Giorgione (1505).

Righteous as he was, Berenson turned the money down and attributed the painting to Titian. It was later discovered that the painting was in fact a genuine Giorgione, and even a connoisseur as great as Berenson could make a grave and costly mistake such as this.

Although it places excessive reliance on experts and their opinions, the art of connoisseurship still continues to thrive until this present day. It still serves as a vital part in the authentication of artworks.

2.3 Automatic Characterization

Automatic characterization can be achieved by looking at the painting as a whole or as a composition of its formal elements. This subsection outlines the methods used in both approaches for the automatic characterization of paintings.

2.3.1 Whole Painting Characterization

The work of Gatys, Ecker, and Bethge (2015) took paintings as whole, successfully identified their characteristics and transferred the styles into photographic images. Their work used a Convolutional Neural Network (CNN) which has the ability to separate the style and content of paintings. As a biologically inspired vision model, CNN has demonstrated a near-human performance in recognizing object and faces. It consists of layers of computational units that are used for processing visual information. The information is processed in a feed-forward and hierarchical fashion. Each layer is a set of image filters for extracting features from the input image. Each of the layers produces different feature maps, which is the filtered input image. The authors identified the images' style using a feature space obtained from the correlation between filter responses in each of the network layer.

FIGURE 2.2: An example from the work done by Gatys, Ecker, and Bethge (2015).

Similar to the work by Gatys, Ecker, and Bethge (2015), Chu and Wu (2018) explored deep correlation features for classifying painting styles. They determined the Gram-based correlation (Gatys, Ecker, and Bethge, 2015) between the feature maps and formulated it as a style representation. After the Gram matrix is formed, it was traversed by raster scan and transformed into a style vector. From the traversal, a 512x512 image was converted into

262,144-dimensional deep correlation feature vectors. In addition to the Gram-based vectors, other statistical features are also computed from the feature maps. Those other features are: Pearson correlation, Spearman correlation, covariance, Chebychev distance, Euclidean distance, and cosine similarity. The combined vectors were then classified using SVM and produced the average accuracy of 70.99% in differentiating 17 painting styles.

The work of Hughes, Graham, and Rockmore (2010) used machine learning for characterizing artworks by the Flemish painter Peter Bruegel the Elder. They used sparse coding analysis for distinguishing authentic Bruegel paintings from imitations by determining their sparse model similarity. The sparse model describes the image space by training a set of orthogonal basis function that will serve as a building block to define the image space. Sparse coding is an effective method for representing features in two dimensional images because of the images sparseness of statistical structures that are considered to give a high contribution to the perception of similarity.

Sener, Samet, and Sahin (2012) used the image processing approach in artistic style characterization by extracting various features for identifying children's book illustrators. The characterization is done for illustrators such as Alex Scheffler, Debi Gliori, Dr. Seuss, and Korky Paul. From those illustrators, Sener, et al. extracted features such as 4x4x4 bin RGB histograms, GIST (Douze et al., 2009), dense SIFT (Lowe, 2004), and gradient histograms (HoG). After the extraction, the features are tested by classification using Support Vector Machine with various kernels. The tested features are successful in distinguishing one artist's style from another.

Agarwal et al. (2015) classified paintings from six different genres and ten different styles using various features such as dense SIFT (Lowe, 2004), gist (Lowe, 2004), histogram of gradients (HoG), local binary pattern (LBP)

(Pietikäinen, 2010), grey level co-occurence matrix (GLCM) (Haralick, Shanmugam, and Dinstein, 1973), and colour. The classification is done using the LibSVM classifier (Chang and Lin, 2011) in WEKA with χ^2 kernel. They found that SIFT is an ideal feature for classifying landscape and portrait paintings and also the most descriptive of all their features. While the classifications generated the accuracy of 84.56%, their features were not robust enough to classify paintings from the same art movement. For instance, they found that surrealist paintings are often classified as pop-art paintings since they both belong to the modern art movement.

In contrast to the works above, the artistic style characterization presented in this thesis examined images as compositions of their particular formal elements, which in this case consist of brushstrokes. The characterization combines image processing and machine learning techniques to extract features from brushstrokes in digital paintings. Since extracting brushstrokes can be a laborious job, this work focused on extracting the visible brushstrokes. After the visible brushstrokes are extracted, their properties such as shape and texture features are obtained. Then, machine learning is used to identify the important features that define the style.

2.3.2 Characterization by Identifying the Formal Elements

Brushstrokes

Brushstrokes are the medium used by painters to communicate what they want to convey in their paintings. The way they are drawn can also provide some information related to the painter, for instance the painter's art movement and even his/her emotional state (Callen, 1982). Due to this fact, brushstroke extraction has an important role in the area of digital painting

analysis since brushstrokes contain a lot of information that can be used as features to represent a painting.

Jiang et al. (2006) distinguished two traditional Chinese paintings genres, Gong Bi and Xie Yi, from each other using low-level image features. Gong Bi paintings consist of elaborate details and intricate brushstrokes, while the simpler Xie Yi paintings show exaggerated and free-handed brushstrokes. The features that they used include the Ohta colour histogram (Ohta, Kanade, and Sakai, 1980), colour coherence vector (CCV) (Pass, Zabih, and Miller, 1997), and their novel method called edge size histogram (ESH). They used HSL colour space with the consideration of colour, saturation, and luminosity being the three aspects that artists use to create their works. Their classification result using SVM yielded the accuracy of 95.56% when the combined features were used and 85.29% when only ESH features are used.

a b

FIGURE 2.3: Traditional Chinese paintings in: (a) Gong Bi, and (b) Xie Yi style.

In their research of characterizing and classifying Chinese ink wash paintings, Sheng and Jiang (2013) performed an examination of the local and global features of the paintings. The features are obtained from the distribution of the lines and brushstrokes. They calculated greyscale histograms (Şengür and Guo, 2011) from both the entire image and local regions of the

painting. The histogram obtained from the entire image is considered as the global feature, while the one from local regions of the painting is considered as the local feature. The features they selected can differentiate the works of five Chinese ink wash painters. The experiments yielded the average precision and recall of 0.828 and 0.820 for the classifications using combined global and local features.

Li et al. (2012) extracted physical features of brushstrokes from paintings by Vincent van Gogh to differentiate his periods of works. In their research, a painting is represented as a series of statistical brushstrokes features. The features are derived by the influence of art historian who suggested that brushstroke properties are highly correlated with a particular painting era. Suppose we have brushstroke i with the center coordinate (u_i, v_i) where u_i is the average vertical positions and v_i is the average horizontal positions of all pixels in the brushstroke. If we have the target image I with C numbers of columns and R numbers of rows, the pixel coordinate is given as (u, v) where $u = 0, 1, ..., R - 1$ and $v = 0, 1, ..., C - 1$. The statistical brushstroke features that are computed from the image are:

1. Number of brushstrokes in the neighbourhood (NBS-NB): A brushstroke i is defined as the neighbour of another brushstroke j if $|u_i - u_j|$ and $|v_i - v_j|$ are less than the threshold s.

2. Number of brushstrokes with similar orientations in the neighbourhood (NBSSO).

3. Orientation standard deviation for brushstrokes in the neighbourhood (OSDNB).

4. Size: The number of pixels in the brushstroke.

5. Length: The number of pixels along the medial axis of the brushstroke.

6. Broadness: The average Euclidean distance on the image plane from a boundary pixel to the medial axis in the brushstroke.

7. Broadness homogeneity: The standard deviation of the distance between every boundary pixels to the medial axis in the brushstroke.

8. Straightness: the absolute value of the linear correlation between the horizontal and vertical coordinates of the pixels on the brushstroke's medial axes.

9. Elongation: The ratio between length and broadness

10. Orientation (Russ, 2015): Suppose we have a brushstroke B with size N and pixel coordinates (u_i, v_i) with $i = 1, 2, \ldots, N$. The orientation of B is:

$$\begin{cases} \pi/2 & m_{u,v} = 0 \\ arctan\frac{m_u - m_v + \sqrt{(m_u - m_v)^2 + 4m_{u,v}^2}}{2m_{u,v}} & otherwise \end{cases} \tag{2.1}$$

where

$$\begin{aligned} m_u &= \sum_{i=1}^{N} u_i^2 - \frac{1}{N}(\sum_{i=1}^{N} u_i)^2 \\ m_v &= \sum_{i=1}^{N} v_i^2 - \frac{1}{N}(\sum_{i=1}^{N} v_i)^2 \\ m_{u,v} &= \sum_{i=1}^{N} u_i v_i - \frac{1}{N}\sum_{i=1}^{N} u_i \sum_{i=1}^{N} v_i \end{aligned} \tag{2.2}$$

Berezhnoy, Postma, and Van Den Herik (2009) developed a model called prevailing orientation extraction technique (POET). This method extracted brushstroke texture orientation for the segmentation of individual brushstrokes of Van Gogh. The method consists of two stages, which are the

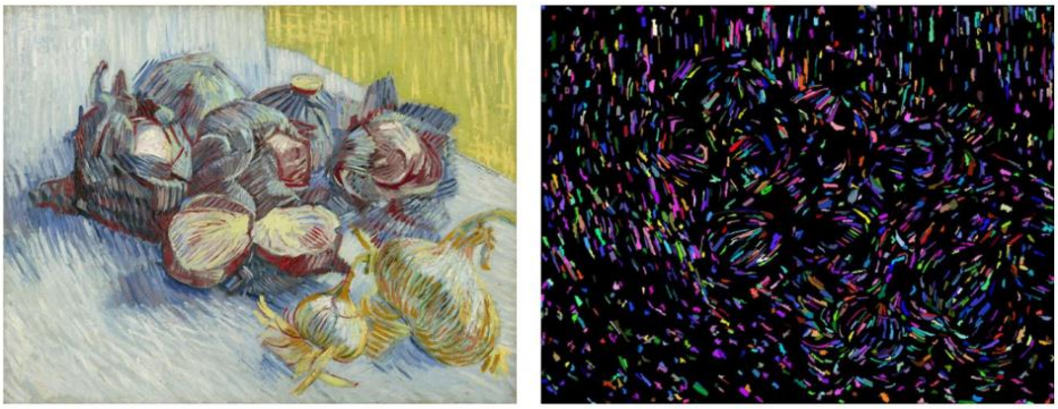

a b

FIGURE 2.4: The result from brushstroke extraction algorithm developed by Li et al. (2012). (a) The original painting, and (b) the extracted brushstrokes.

filtering and orientation extraction stage. In the filtering stage, a rotation-invariant circular filter with good response for band-passing was applied. Meanwhile, the orientation extraction stage obtained the principal orientation of brushstrokes from the filtered image. The filtered images were transformed into binary images using multilevel thresholding before the orientations were extracted. The evaluation of POET is based on the cross comparison between judgement of POET and human subjects.

Research done by Johnson et al. (2008) explores a mathematical analysis for the classification of Van Gogh paintings by analysing the texture of his brushstrokes. They examined high resolution greyscale scans of 101 paintings consisting: eighty-two paintings by Van Gogh, six paintings by other painters, and thirteen other paintings which are debatable to be Van Gogh or non-Van Gogh according to art experts. They used edge detection to extract visible brushstrokes from the paintings, and then derive the geometric features. In addition, they also extract the brushstrokes' texture-based features using wavelets. They argued that the accurate extraction of visible brushstrokes is a very challenging task that needs to be explored further.

Other Formal Elements

Aside from brushstrokes, other formal elements can also play an important role in representing style. Lee and Cha (2016) categorized paintings by first identifying their colour and composition features. The colour features that were used are the average of hue and saturation, the number of hues, and the hue distribution. The composition features are described as shape and colour features of the top three largest regions with dominant colours extracted by K-means clustering. They did binary classifications between two different genres of paintings: expressionism and impressionism, expressionism and post-impressionism, expressionism and surrealism, impressionism and post-impressionism, impressionism and surrealism, and post-impressionism and surrealism. The experiments which are done using self-organizing map (SOM) (Kohonen, 1998) yields the highest precision of 0.95 which were given by the classification between expressionism and impressionism, each of them being very different to each other visually. The lowest precision was 0.85 which were given by the classification between impressionism and post-impressionism, two genres which are connected through the similar use of vivid colours, thick application of paint, and real-life subject matter.

Icoglu, Gunsel, and Sariel (2004) performed a classification between three artistic movements using light features such as the percentage of dark colours, the properties of luminance histogram, and the grey scale distribution. Their classification using Bayes, K-nearest neighbour, and SVM yielded a maximum accuracy of 95%. Another similar study is done by Kroner and Lattner (1998), who analyzed the light features of freehand drawings. Their contributions including the eight bins black-and-white-ratio histogram which measured the ratio between black and white pixels in the image. They formulated three light features from the histogram, which are: the difference

between the third and fourth bin, the division product between the fifth and fourth bin, and the multiplication product of the first and fourth bin.

One of the most significant findings in the research area of artistic style characterization is the work by Taylor, Micolich, and Jonas (1999). He successfully characterized the seemingly random artwork of Jackson Pollock into discrete features by calculating their fractal dimension using box counting method. From their investigation, it was shown that Pollock's works yield a fairly constant fractal dimension between 1 to 1.72. Because of this finding, they claimed that fractal analysis can be used as a quantitative and objective method to authenticate Pollock's paintings.

FIGURE 2.5: "Autumn Rhythm (1950) by Jackson Pollock, which has an estimated fractal dimension of 1.67.

Chapter 3

System Framework

3.1 Introduction

This chapter presents the details of various processes used in our artistic style characterization system. Subchapter 3.2 describes the four classes used for the classification algorithm, along with each of their examples of input image patches. Subchapter 3.3 presents the constituent steps of the characterization. All the preprocessing methods that are used before the characterization stage, including colour space conversion and image filtering, are outlined in Subchapter 3.4. Segmented brushstroke regions are computed using four methods in Subchapter 3.5. These methods perform feature extraction and selection, which are described in Subchapters 3.6 and 3.7.

3.2 The Dataset

A dataset with four classes are used in this research. They are chosen with the consideration of their varying degrees of similarity with the works of Van Gogh. Rembrandt's style is completely different from Van Gogh, while the Impressionists' thick application of paint and vivid colour is similar to

Van Gogh. Cuno Amiet, meanwhile, was influenced by Van Gogh since they are both Post-Impressionists.

The paintings in each dataset are processed as images with the size of 500x500 pixels by MATLAB's block processing module `blockproc`. Block processing was chosen after considering the very large size of the paintings. This process is necessary to prevent large processing overheads resulting from high resolution images in our datasets. The process in non-overlapping, which means that each images are mutually exclusive with one another. In the case of when the painting size is not a multiple of 500, the block processing will use zero padding to extend the size of the patch to 500x500. We did this to retain the remaining regions of the painting that may contain useful information. The padded region will be filtered out in the outlier removal process.

FIGURE 3.1: Zero padded regions which are the residue of the patch division process.

1. **Vincent van Gogh (1853-1890)**

FIGURE 3.2: The sample images in Van Gogh class.

TABLE 3.1: The Van Gogh Class.

Title	Year	Period	Resolution
Le Moulin de la Galette	1886	Paris	3840x3082
Self-Portrait with Grey Felt Hat	1886	Paris	2606x3163
Self-Portrait with Straw Hat	1887	Paris	2452x3068
Cabbages and Onions	1886	Paris	3840x2975
A Pair of Leather Clogs	1889	St. Rémy	3840x3034
The Garden of Saint-Paul Hospital	1889	St. Rémy	3840x3039
Landscape at Twilight	1890	St. Rémy	3507x1719
Tree Roots	1890	St. Rémy	3840x1879
View of Auvers	1890	St. Rémy	3840x3694
Wheat Fields	1890	St. Rémy	3840x3153
Wheat Field under Thunderclouds	1890	St. Rémy	3840x1885
Wheat Field with Crows	1890	St. Rémy	3840x1939

Our main research interest is Vincent Van Gogh, a Dutch Post-Impressionist painter. His subject matters were rendered by thick, rhythmic brushstrokes known as *impasto*. In his paintings, colours were used for capturing mood rather than be used realistically. Hence, Van Gogh's subject matters are independent from his colours. His 2,000 paintings include portraits, self-portraits, landscapes, and still lifes (McQuillan, 1989).

2. **Rembrandt Harmenszoon van Rijn (1606-1669)**

   Rembrandt is a Dutch master whose works includes a wide range of scenes and subject matter, including portraits, self-portraits, and biblical and mythological scenes. As a Baroque-Realist, Rembrandt's paintings have blended strokes which aim to portray the subject matter as realistically as possible. His subject matters are depicted in rich details, for instance, in elaborate costumes and jewellery.

   His portraits have the ability to create a narrative by incorporating a particular angle of gaze on his subject (DiPaola, Riebe, and Enns, 2010). In addition, contrasting light and shadows were emphasized to achieve a more dramatic effect.

FIGURE 3.3: The sample images in Rembrandt class.

TABLE 3.2: The Rembrandt Class.

Title	Year	Resolution
Parable of the Hidden Treasure	1630	3703x2864
The Entombment of Christ	1635-1639	2024x1604
Judas Returning the Thirty Pieces of Silver	1629	2048x1585
The Apostle Paul in Prison	1627	3168x3727
David with the Head of Goliath before Saul	1627	2048x1412
Balaam and the Ass	1626	2252x3000
Man in a Gorget and a Cap	1626-1627	2358x3208
The Spectacle-Pedlar	1624-1625	2793x3284
The Operation	1624	1410x1724
The Abduction of Europa	1632	3000x2342
The Raising of Lazarus	1630-1632	4113x4905
The Parable of Rich Fool	1627	2998x2228
Tobit Accusing Anna of Stealing the Kid	1626	2058x2724
Family Portrait	1665	3000x2264
Descent from the Cross	1633	2789x3840
The Stoning of Saint Stephen	1625	2024x1458

3. **The Impressionists**

   Impressionism was an artistic movement that began in nineteenth-century France. Impressionist paintings are characterized by seeking to capture life as if viewed 'at a glance', rather than laborious realism. The Impressionists used thick, disconnected, rhythmic brushstrokes to convey a sense of movement in their works (Rubin, 1999). They paid extra attention to the fleeting effects of light, atmosphere and movement. The subject matters that were popular among the Impressionists are landscapes, still life, and scenes in modern life, especially of bourgeois, leisure, and recreation.

FIGURE 3.4: The sample images in Impressionist class.

TABLE 3.3: The Impressionists Class.

Title	Painter	Year	Resolution
At the Water's Edge	Paul Cézanne	1890	4000x3146
Bazille and Camille	Claude Monet	1865	2975x4000
Flowers in a Rococo Vase	Paul Cézanne	1876	2452x3068
Oarsmen at Chatou	Auguste Renoir	1879	4000x3255
Sainte-Adresse	Claude Monet	1867	4000x2786
The Japanese Footbridge	Claude Monet	1889	4000x3219
Woman with a Parasol	Claude Monet	1875	3220x4000

In this research, the works of Claude Monet, Paul Cézanne, and Pierre Auguste Renoir are used due to their high influence within the movement.

4. **Cuno Amiet (1868-1961)**

   Cuno Amiet was a Swiss Post-Impressionist and Expressionist. He was a pioneer of modern art in Switzerland, producing more than 4,000 paintings. Nearly a quarter of these paintings were self-portraits. His paintings are characterized by bold strokes and use of vibrant, contrasting colours, especially between 1940-1950 in his later years (Chilvers and Glaves-Smith, 2009). His subject matters were emphasized in geometric form, distorted to display expressive effect.

Every painting in the dataset is in high resolution. The names of the datasets with each respective number of images are given in Table 3.5.

FIGURE 3.5: The sample images in Cuno Amiet class.

TABLE 3.4: The Cuno Amiet Class.

Title	Year	Resolution
Morning Mood	1932	4000x3151
Rose Garden	1935	4000x3223
Rosebush After Thunderstorm	1933	2910x4101
Summer Landscape	1956	4000x3285
While Cyclamen	1955	3273x4000
Zinnias on Blue Cloth	1944	4000x3241

TABLE 3.5: The Four Classes in the Dataset

Name of Painter	Class Name	# Paintings	# Images
Van Gogh	VG	12	377
Rembrandt	R	16	326
Monet, Cézanne & Renoir	IMP	7	286
Cuno Amiet	CA	6	275

3.3 The Characterization Process

The artistic style characterization algorithm is described as follows:

1. Divide each painting in the VG dataset into images of 500x500 pixels.

2. Identify the visible brushstrokes from each image by filtering out regions in the image that are not prominent.

3. Extract shape and texture features from the visible brushstrokes. Every brushstroke in the image p has a feature set of $F_p = \{f_1, f_2, ..., f_n\}$.

4. Perform feature selection. For each brushstroke p, the selected feature set is $S_p = \{f_1, f_2, ...f_m\}$ where $S_p \subseteq F_p$. The overall feature set of class

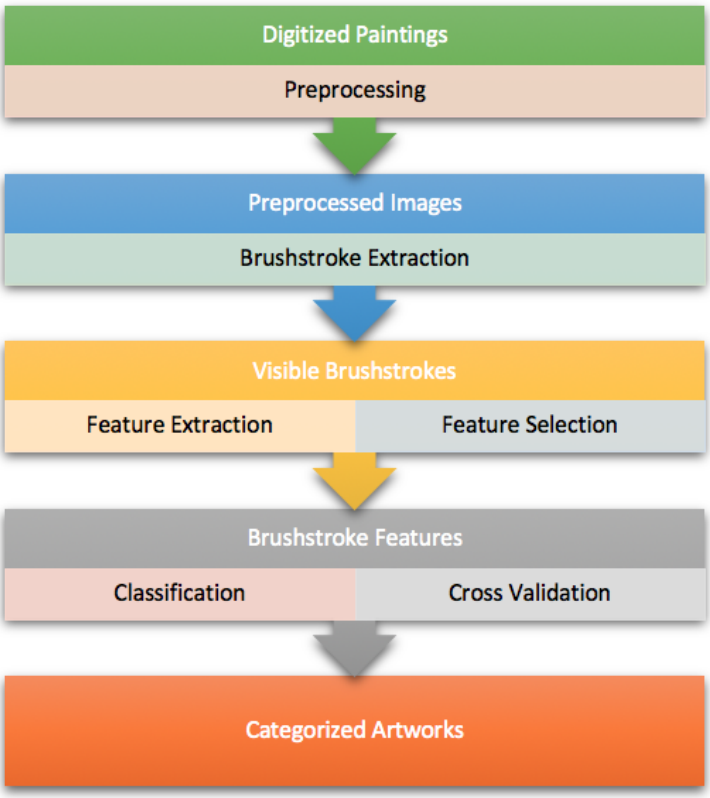

FIGURE 3.6: The framework of the artistic style characterization system

Van Gogh in the dataset is denoted as $S = \{S_1, S_2, ..., S_i\}$ where i is the number of brushstrokes in the dataset. The process of feature selection will be discussed later in Subchapter 3.7.

5. Repeat the previous four steps for the classes R, IMP, and CA. For each brushstrokes p, the obtained feature set is $T_p = \{f_1, f_2, ..., f_m\}$. The overall feature set of the testing datasets is denoted as $T = \{T_1, T_2, ..., T_j\}$ where j is the total number of brushstrokes in the datasets.

6. Do a classification-based test from both S and T to measure the representability of the feature subsets in S.

7. Perform a cross validation technique to determine whether the classification is able to generalize its result to an independent dataset.

3.4 Preprocessing

Before performing the classification, we did several preprocessing operations, which are given in the subsections below.

3.4.1 Colour Space Conversion

In this research, we convert the colour space of the digital paintings into CIELAB colour space. CIELAB, also known as L*a*b colour space, is created to be *perceptually uniform* with the human vision. The amount of numerical change in CIELAB components correlates with the amount of perceptual change in the human eye. It has three components:

1. L which represents lightness. CIELAB's L component closely matches human perception of lightness.
2. a which represents the green-red component of the colour hue.
3. b which represents the blue-yellow component of the colour hue.

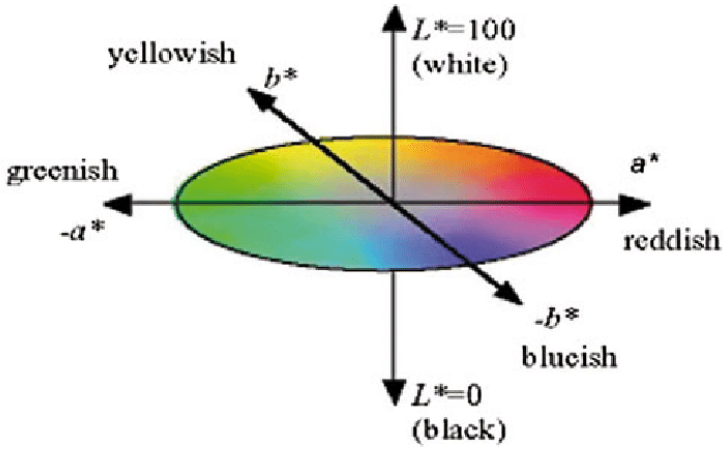

FIGURE 3.7: The CIELAB colour space

CIELAB is widely used because the L*a*b space itself has bigger number of gamut of computer displays and printers. It is also copyright and license-free.

3.4.2 Image Filtering

Region extraction is a delicate process in image processing due to the existence of noise within the image. In order to minimize or eliminate the effect of noise, many smoothing algorithms are performed as a preprocessing step before the image regions are extracted. In this research, we use a circular filter in conjunction with our brushstroke segmentation algorithms

In their work, Berezhnoy, Postma, and Van Den Herik (2009) suggested circular filter, a variety of median filter with a circular neighbourhood of diameter d as an effective preprocessing filter for enhancing parallel contours of the brushstroke. The neighbourhood diameter d corresponds to the average separation of the parallel contours of the brushstrokes. The formula for circular filter is given in Equation 3.1.

$$p'(m,n) = median\{p(i,j)|i,j \in N\} \tag{3.1}$$

$p'(m,n)$ is the filtered pixel with the coordinate (m,n) in the image and N is the circular neighbourhood with diameter d around (m,n).

In this work, circular filter has successfully magnified the outline of Van Gogh's brushstrokes, thus enhancing the result of visible brushstroke segmentation. It has also remove noise and unnecessary details, such as streaks inside the stroke and concealed strokes which lie behind the visible strokes. The effect of circular filter in Van Gogh's brushstroke segmentation can be seen in Figure 5.9.

3.5 Visible Brushstroke Extraction

In this subchapter, four methods for brushstroke region extraction are outlined. These methods had been implemented independently and their analysis is provided in Chapter 5. We limit the extraction to the visible brushstrokes that can be clearly identified - in other words, brushstrokes that are not located behind any other brushstrokes.

3.5.1 Iterative Extraction Method

A brush region in a painting is characterized by a high level of homogeneity in colour values. Region extraction is often done through recursive connected component labelling. The brushstroke region extraction algorithm introduced in this thesis is iterative. Thus, it simultaneously generates the medial axis of a brushstroke region and identifies the region itself.

Before we proceed to extract brushstrokes using this method, we filter the images with circular filter to smoothen the image and magnify the brushstroke's rounded corners. In this method, a circular blob of uniform colour is used as a template and its corresponding regions are iteratively computed, with the locus of the blob centroid forming a medial axis. This medial axis is then referred as a brush path. More formally, B_R, a blob of radius R with centre at pixel location P_0 in image space I is given as follows:

$$B_R(P_0) = \{P \in I : ||P - P_0|| \leq R\} \tag{3.2}$$

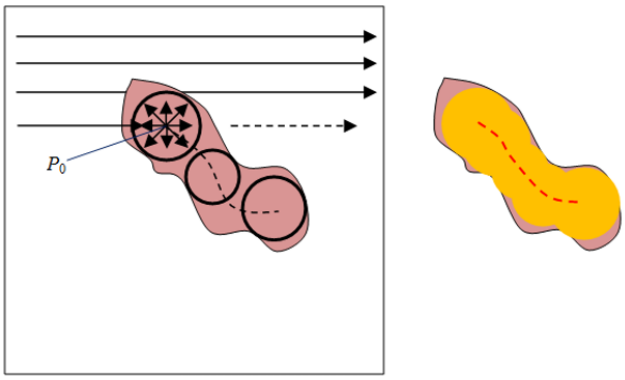

FIGURE 3.8: The sequential blob matching of a sample brush-stroke region.

The uniformly-coloured region S_R centered at P_0 is expressed as a subset of $B_R(P_0)$ with the constraint of:

$$\begin{aligned} S_R(P_0) = P \in B_R(P_0) | |v(P) - v(P_0)|| \leq \Delta E \\ size(S_R(P_0)) \geq 0.9(size(B_R(P_0))) \end{aligned} \tag{3.3}$$

Where $v(P)$ is the vector of CIE colour components at pixel P and ΔE is the error threshold for colour comparison, as given in Equation 3.3. The function size denotes the number of pixels in a set. The second condition in Equation 3.3 specifies the colour comparison condition for the blob. A region is considered to be a homogeneous region if 90% of the pixels in the set S_R is in a similar colour. The blob template is moved over the canvas in a sequential left-to-right, top-to-bottom manner with the largest possible brush radius R until a matching region is found.

The blob is moved to its eight nearest neighbours. Two pixels are 8-neighbours if they share at least one corner between them (Jain, Kasturi, and Schunck, 1995). The movement allows a variation of the radius from R down to $R-10$. The blob will travel to a direction that gives the maximum blob radius that

fits the region with respect to the constraints given in Equation 3.3. This implementation of an adaptive blob size for a greedy path selection becomes the main aspect of the extraction algorithm. Visitation marking of the blob centroids is done to avoid revisiting the same point in a subsequent iteration. The extraction of one skeleton is finished when a blob within the specified radius $[R - 10R]$ is not found in the next step. In this stage, all pixels inside the matched blob regions will be marked as visited. The search for the next blob location resumes at the next unvisited pixel found with the left-to-right, top-to-bottom manner mentioned earlier.

The scanning of a whole image is done by repeatedly replacing R with a lower value ΔR where ΔR is the step size of 2 pixels. The overall extraction will terminate after we have reached last brush in the brush set. Note that in each iteration, more and more pixels are marked as visited and therefore the processes for lower values of R takes progressively lesser computational time.

The colour difference between two pixels $P_i(L, a, b)$ and $P_j(L', a', b')$ constraint for the blob scanning process is given as follows:

$$||P_i - P_j||^2 = (L - L')^2 + (a - a')^2 + (b - b')^2 < 9 \tag{3.4}$$

Where L, a and b are the colour values of a pixel P_0, and L', a' and b' values of a pixel P_1.

One problem that may arise in the extraction process is colour discontinuity within regions. This problem is caused by the use of a single colour value of P_0 as the reference for the extraction of the entire brush region. It can be solved by the continual update of the colour reference using the average of matched colour values of the current blob position during the iterations.

3.5.2 Neutrosophy Based Segmentation Method

Neutrosophy is a branch of philosophy introduced by Florentin Smarandache in 1980. It comes from the Latin word *neuter* which means 'neutral' and the Greek word *sophia* which means 'wisdom'. Neutrosophy takes three things to be considered: A, which denotes a proposition, theory, event, concept or entity; *Anti-A*, which denotes the opposite of A; and *Neutral-A*, which is neither A or *Anti-A* (Smarandache, 1999).

Neutrosophic logic is the generalization of Fuzzy Logic based on the principles of neutrosophy. Each proposition P in the logic is estimated to have constituent percentages of truth (T), falsehood (F), and indeterminacy (I), with the sum of T, F, and I being 100%. The percentage of indeterminacy I is introduced to take into account the unexpected parameters that are hidden in some of the propositions. The application of neutrosophic logic can be found in various fields of research such as probability theory, robotics, and also image processing. The introduction of indeterminate elements can be applied for image denoising and enhancement, which is beneficial for various image processing applications, such as medical image analysis and artistic style characterization.

Research done by Şengür and Guo (2011) combined features from wavelet decomposition and neutrosophic membership value to perform image segmentation. Their research applied one-level wavelet decomposition to the greyscale image. They also calculated the mean of energy in a window on the wavelet coefficients to capture the characteristics of the local texture. The calculated features are then all combined for g-K-means clustering. Their proposed method is proven to be more efficient than mean shift filtering in higher dimensional space (MSF-HDS) (Ozden and Polat, 2007) and Waveseg (Jung and Scharcanski, 2005).

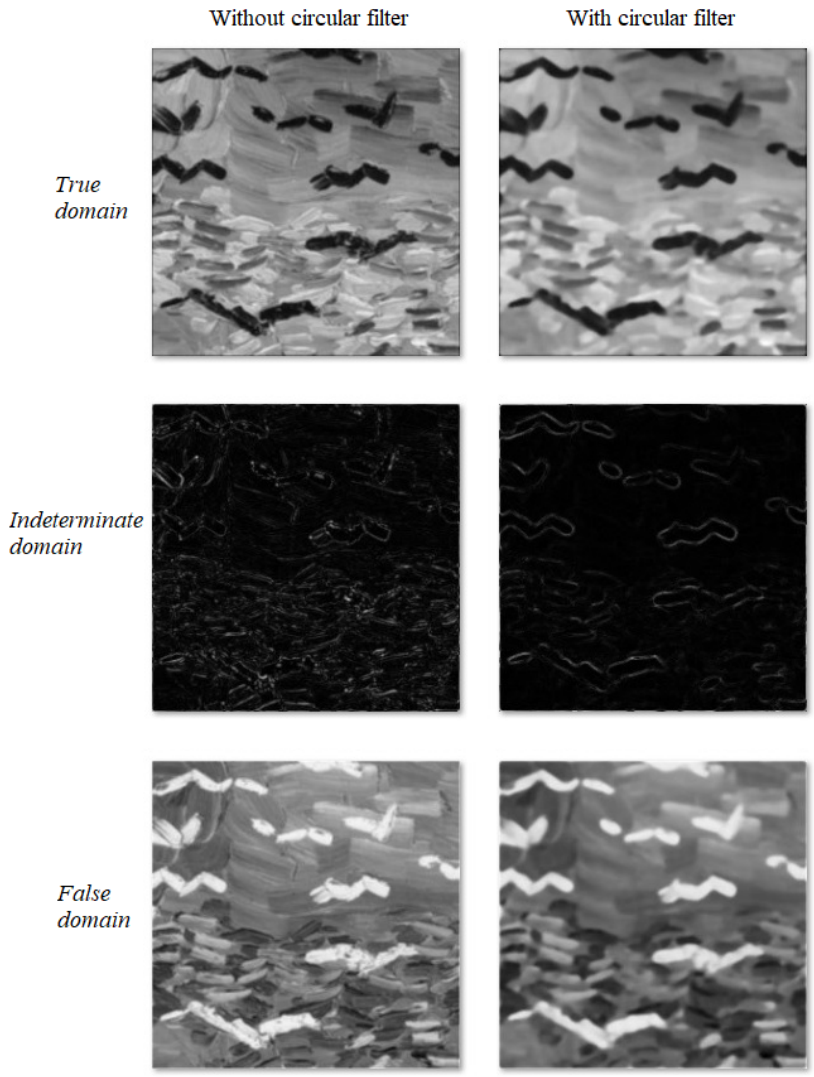

FIGURE 3.9: The effect of applying circular filter that is seen in true domain $T(i, j)$, indeterminate domain $I(i, j)$, and false domain $F(i, j)$.

In their other works, Guo and Şengür (2014) explored a novel image segmentation by defining a neutrosophic similarity function in the pixel clustering objective function. They identified that image noise can be seen as indeterminate pixels and can be removed by eliminating those pixels from the original image. They proposed a method called neutrosophic set clustering (NSC), a K-means clustering based version of the original neutrosophic set method. To segment the image using NSC, they first converted the image to

the neutrosophic set domain and computed the value of neutrosophic similarity function for each pixel under three conditions: the pixel's gradient, homogeneity value, and intensity value. The pixels are then clustered by minimizing the K-means objective function value with respect to the neutrosophic similarity function. The pixels in the same cluster belong in the same region.

We converted the image into a binary image and define it in neutrosophic domain. A pixel $P(i, j)$ in a binary image is defined in the neutrosophic domain as:

$$P_{NS}(i, j) = T(i, j), I(i, j), F(i.j) \tag{3.5}$$

$T(i, j)$ is the probability of $P(i, j)$ belongs to the white pixel set, $F(i, j)$ is the probability of $P(i, j)$ belongs to the black pixel set, and $I(i, j)$ is the probability of $P(i, j)$ belonging to the indeterminate pixel set which is neither white or black.

$T(i, j), F(i, j)$, and $I(i, j)$ are called *membership value* and are computed using these following equations:

$$T(i, j) = \frac{\hat{g}(i, j) - \hat{g}_{min}}{\hat{g}_{max} - \hat{g}_{min}} \tag{3.6}$$

$$I(i, j) = \frac{\delta(i, j) - \delta_{min}}{\delta_{max} - \delta_{min}} \tag{3.7}$$

$$\delta(i, j) = |g(i, j) - \hat{g}(i, j)| \tag{3.8}$$

$$F(i, j) = 1 - T(i, j) \tag{3.9}$$

The value of $g(i,j)$ represents the intensity of a pixel in coordinate (i,j). $\hat{g}(i,j)$ is the local mean value of the neighbourhood of (i,j) with $\hat{g}_{max}$ and $\hat{g}_{min}$ as its maximum and minimum value.

3.5.3 Texture Boundary Detection Method

This method detects brushstrokes by identifying different textures in the painting image. A brushstroke can have a very different texture from other neighbouring brushstrokes. This happens due to various factors, such as artistic preferences, paint concentration, stroke orientation, and so forth. This method uses image entropy to measure the randomness of the pixel information stored in every visible brushstroke.

To obtain the visible brushstrokes area from the image I, we perform these steps:

1. Read the image I and convert I to grayscale image I_{gray}.
2. Adjust the contrast of I_{gray} using histogram equalization.
3. Perform entropy filtering (Yan, Sang, and Zhang, 2003) for every pixel in I_{gray}. The result of this process will be called as I_{ent}.
4. Perform DBSCAN clustering (Kovesi, 2000) to mask the regions with significant entropy change in I_{ent}. The ϵ is chosen using the nearest neighbour graph which plots the distance to $k = minPts - 1$ ordered from the largest to the smallest value (Schubert et al., 2017).
5. The isolated image regions is called as $I_{grayvis}$.

The formula for entropy in pixel P is given as follows:

$$E_p = -\sum(n_P log_2 n_P) \tag{3.10}$$

where n_P is histogram counts of the neighbourhood of P. In this method, the neighbourhood of $9x9$ is used.

3.5.4 Gabor Filter Based Segmentation Method

In this method, a filter bank of Gabor filters with various scales and rotations is applied to every image patch in order to evaluate its distribution of intensity level. Gabor filters are proven to be a robust method for analysing oil painting images which have textured brushstrokes (Putri and Arymurthy, 2010).

The two-dimensional Gabor filter is defined as:

$$g_{\lambda,\theta,\sigma,\phi}(s,t) = e^{-(\frac{s'^2}{\sigma_s^2}+\frac{t'^2}{\sigma_t^2})} cos(\frac{s'}{\lambda}+\phi) \tag{3.11}$$

where $s' = s\,cos\,\theta + t\,sin\,\theta$ and $t' = -s\,sin\,\theta + t\,cos\,\theta$. From Equation (3.11), a filter response of signal f is defined as:

$$R_{\lambda,\theta,\sigma,\phi}(x,y) = \iint_W f(x-s, y-t) g_{\lambda,\theta,\sigma,\phi}(s,t)\,ds\,dt \tag{3.12}$$

where W is the filter window, λ is the scale (also known as *spatial frequency*), θ is the orientation, σ_s and σ_t are the standard deviations of Gaussian envelope, and ϕ is the phase offset for the real ($\phi = 0$) and imaginary ($\phi = \frac{\pi}{2}$) components of the filter response (Zang, Huang, and Li, 2013). In this work, the circular Gaussian envelope with $\sigma_s = 1$ and $\sigma_t = 1$ is used.

For every pixel $p(x,y)$ in the painting patches, the Gabor energy is defined as:

$$e_{\lambda,\theta}(x,y) = \sqrt{R_{\lambda,\theta,1,0}(x,y)^2 + R_{\lambda,\theta,1,\frac{\pi}{2}}(x,y)^2} \tag{3.13}$$

The Gabor energies given in Equation (3.13) are computed for $\lambda_i, i = (1, ..., 6) * \sqrt{2}$ and $\theta_j = \frac{j\pi}{8}, j = 0, ..., 7$. Each possible pair of these two parameters λ_i and θ_j are stored in a filter bank.

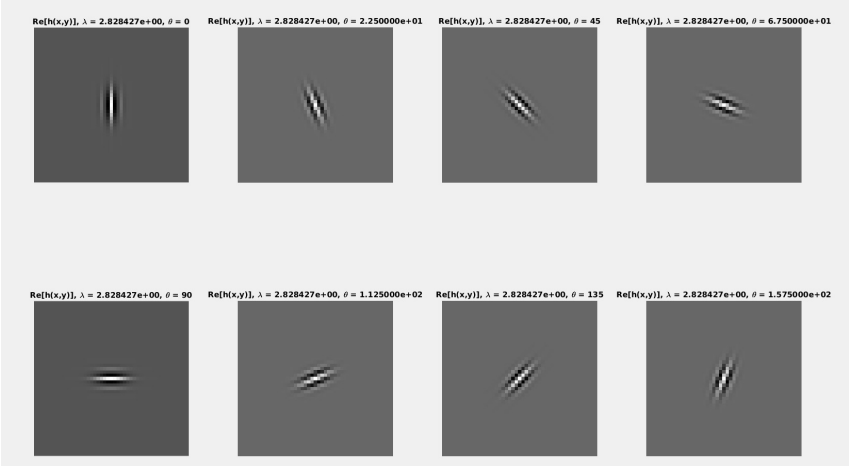

FIGURE 3.10: Visualization of the Gabor filter bank for scale $2\sqrt{2}$ and eight orientations.

Every Gabor filter in the filter bank detects the image intensity transition via convolution. Every convolution will produce energy values for each pixel. The total energy from every convolution in one painting patch is the number of contours (or light-dark transition), thus will detect regions with different textures (Johnson et al., 2008).

The process of Gabor-based visible brushstroke segmentation is outlined below:

1. For each pixel $p(x, y)$ in the input image, compute the array $G_{(x,y)}$ of Gabor energies $e_{\lambda,\theta}(x, y)$ for every combinations of scale $\lambda_i, i = 1, ..., 6$ and orientation $\theta_j = \frac{j\pi}{8}, j = 1, ..., 8$.

2. Apply Gaussian filter to $G_{(x,y)}$ to filter out local variations.

3. Append the x and y value (the pixel's coordinate) to $G_{(x,y)}$.

4. Standardize $G_{(x,y)}$ to be zero mean, unit variance.

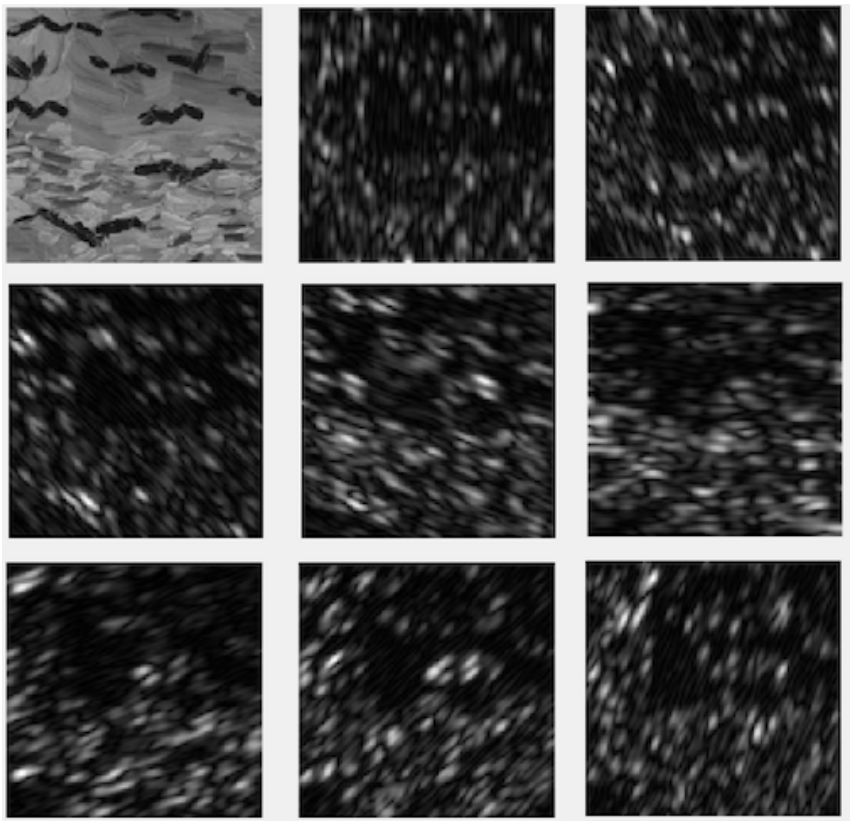

FIGURE 3.11: The visualization of Gabor filter bank in Figure 3.10 when applied to the input image (top left).

5. Group the pixels together using DBSCAN clustering (Ester et al., 1996). Repeat several times until convergent. The pixels that belongs to the same region have similar Gabor energies.

3.6 Feature Extraction

Feature extraction is a process of deriving values from a large dataset that are able to describe the dataset. Ideally, the derived values should be in a much smaller dimension than the dataset itself. They are also required to be non-redundant and able to allow further generalization of the data. A set of features is usually stored in a vector data structure, thus it is called as *feature vector*.

In this thesis, we limit our research scope by extracting two different kinds of low level features which are observed from the paintings' formal elements: Shape and texture. We exclude colour in our observation due to these reasons (Berezhnoy, Postma, and Herik, 2007) :

1. Van Gogh focused on using colours to capture mood and emotion rather than using them in their natural correspondence with the subject matter.
2. Van Gogh's choice of colour varied with his mood and mental state.
3. Van Gogh often purposefully restricted his palette to just a few colours.

3.6.1 Shape

From Van Gogh's visible brushstrokes, we extract the following five features:

1. **Major axis length**. The length of major axis of the ellipse that has the same normalized second order central moments as the region.
2. **Minor axis length**. The length of minor axis of the ellipse that has the same normalized second order central moments as the region.
3. **Eccentricity**. The eccentricity of the ellipse that has the same normalized second order central moments as the region.
4. **Perimeter**. The length of region boundary.
5. **Orientation**. The angle between the x-axis and the major axis.

Those five shape features above are detected from the brushstroke regions using MATLAB's *regionprops* function. Before they are computed, we apply closing operator to close any existing open edges of the brushstrokes. Figure

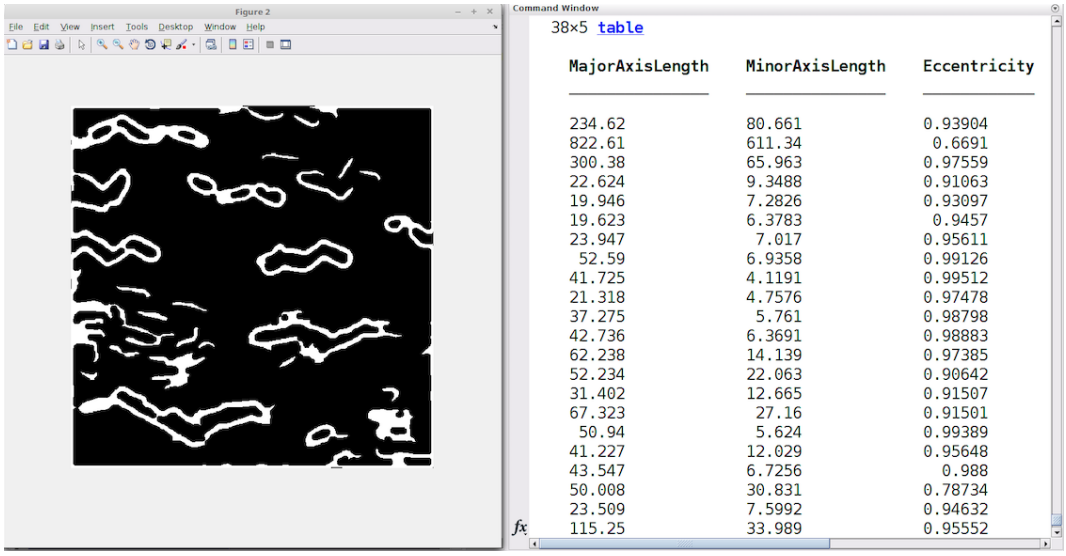

FIGURE 3.12: The detected brushstroke regions and their calculated shape features using MATLAB's *regionprops* function.

3.12 shows the example of extracted brushstrokes using neutrosophy-based segmentation method (see Subchapter 3.5.2) and their shape features.

3.6.2 Texture

After we detect the boundary of the visible brushstrokes using texture boundary detection, we obtain texture features using Gabor filter. Gabor filter has been widely used by computer vision researchers for texture segmentation problems due to its optimal localization properties in spatial and frequency domain (Jain, Ratha, and Lakshmanan, 1997).

In this research, the Gabor energies are calculated for every pixel in every brushstroke with six different scales and eight different orientations. For each brushstroke, the mean and standard deviation for all the Gabor energies are obtained, thus giving us the total number of 96 texture related features. To sum up, 101 features are used for the classification.

3.7 Feature Selection

Before performing any machine learning activities, data size reduction is essential since higher number of features correlates highly to model overfitting. Overfitting is a condition when the statistical inference of the model correlates very highly with the model itself, resulting in the failure to predict future observations. It is considered as a violation of the principle of Occam's Razor, which stated that the right solution of a problem should be the simplest one. In machine learning, an overfitted model is also called as *overtraining*.

Data size reduction can be done by performing feature transformation or feature selection to the dataset. Feature transformation converts the original features in the dataset to new features that are more representable and meaningful (Jović, Brkić, and Bogunović, 2015). Two of the most frequently used feature transformation methods are Principal Component Analysis (PCA) (Pearson, 1901) and Linear Discriminant Analysis (LDA) (Cohen, West, and Aiken, 2014).

Feature selection is a technique for finding a subset of features from the existing features in the dataset. Given a dataset of $M-$dimensional features, feature selection finds a subspace of $m-$dimensional features that best describe the target class. Feature selection aims to improve the performance of machine learning method by removing irrelevant and redundant entities from the feature set. Finding the optimal feature subset for a feature selection problem is considered to be NP-hard (De Silva and Leong, 2015).

There are two kinds of feature selection methods: the filter and the wrapper methods. Filter methods score a feature subset by using an intermediary

measure rather than the error rate. Some of the measures used in filter methods are: inter and intra-class distance (Yang and Pedersen, 1997), Pearson's correlation coefficient (also known as Pearson's r), and relief-based algorithm (Urbanowicz et al., 2017). Wrapper methods use each feature subset for training a predictive model. Then, the feature subsets will be scored based on the error rate of the model. Wrapper methods are more computationally expensive than filter method because it needs to train a new predictive model for each of the feature subset. However, it will eventually capture the optimal feature set for a given predictive model (Guyon and Elisseeff, 2003).

The feature classification that is done in this research used Correlation-based Feature Subset (CFS) evaluation with symmetrical uncertainty correlation measure and best first search to select brushstroke features.

3.7.1 Correlation-based Feature Subset (CFS) Evaluation

This work uses a filter method known as the correlation-based feature subset (CFS) evaluation that was proposed by Hall (1998). The method observes the worth of a feature subset by taking two things into account: each feature's individual predictive ability and degree of redundancy. In other words, a desirable feature subset must have high correlation with the class and low correlation between each other.

The CFS subset evaluation equation is given as follows:

$$M_S = \frac{k\overline{r_{cf}}}{\sqrt{k + k(k-1)\overline{r_{ff}}}} \tag{3.14}$$

In Equation 3.14, the correlation between the feature subset and the class is given by the numerator; and the redundancy of the features in the subset is

given by the denominator. M_S is a merit measurement of the feature subset S with k features. $\overline{r_{cf}}$ is the mean of correlation between the class c and every feature $f \in S$. $\overline{r_{ff}}$ is the mean of inter-feature correlation.

The Pearson's r correlation coefficient between two n-dimensional features $X = x_1, x_2, ..., x_n$ and $Y = y_1, y_2, ..., y_n$ is:

$$r = \frac{\sum_{i=1}^{n}(x_i - \overline{x})(y_i - \overline{y})}{\sqrt{\sum_{i=1}^{n}(x_i - \overline{x})^2}\sqrt{\sum_{i=1}^{n}(y_i - \overline{y})^2}} \tag{3.15}$$

There are three kinds of search strategies that the CFS evaluation can use: forward selection, backward elimination, and best first. The forward selection search strategy starts the search from an empty optimal set O, then greedily adds a new feature to O one at a time. The search will stop when no further addition of features produce a higher merit measurement (computed using Equation 3.14). The backward elimination search strategy is the opposite. It starts with adding all features to O and greedily removes features from O one at a time. Backward elimination will stop when the removal of a feature does not result in a higher merit measurement. The best first search can start with either empty or all features in O. If it starts with empty O set, it moves forward through the search space and adds one feature at a time to O. Else, when the search starts with a full O set, it goes backward through the searrch space and deleting one feature at a time from O. The best first search stops when five consecutive expansions of O do not produce better merit measurement.

The CFS evaluation can also use other methods other than Pearson's r for measuring the correlation. In his Ph.D. thesis, Hall (1998) used three methods, which are the symmetrical uncertainty measure, the minimum description length (MDL), and the relief algorithm. According to his observation, the CFS evaluation with symmetrical uncertainty performed better than the

CFS evaluation with MDL and relief algorithm due to its robustness in dealing with small datasets (Hall, 1998).

3.7.2 Symmetrical Uncertainty

Given the random variables X and Y, the formula of the entropy of Y *before* the observation of X is:

$$H(Y) = -\sum_{y \in Y} p(y) log_2 p(y) \tag{3.16}$$

Then, the entropy of Y *after* the observation of X is:

$$H(Y|X) = -\sum_{x \in X} p(x) \sum_{y \in Y} p(y|x) log_2 p(y|x) \tag{3.17}$$

The information gain is which signifies the additional information of Y given by X is:

$$\begin{aligned} gain &= H(Y) - H(Y|X) \\ &= H(X) - H(X|Y) \\ &= H(Y) + H(X) - H(X,Y) \end{aligned} \tag{3.18}$$

The information gain is a symmetrical measure, which means that the information gain of X after observing Y is equal to the information gain of Y after observing X. Even though the information gain is useful for measuring dependencies of two random variables, it is biased in such a way that features with more values will be deemed to have gained more information than features with fewer values.

Symmetrical uncertainty is introduced to solve the bias of information gain by the value ranging from zero to one. The value of zero signifies that the two random variables X and Y are independent, while the value of one shows that the value of X totally affects the value of Y. The formula of symmetrical uncertainty is given as follows (Witten et al., 2016):

$$SE = \frac{2 * gain}{H(Y) + H(X)} \tag{3.19}$$

Like Pearson's r correlation coefficient, symmetrical uncertainty measures the mutual information between features. It is used for calculating the merit measurement of a feature subset in CFS evaluation for feature selection (see Equation 3.14). According to Hall (1998), symmetrical uncertainty is a better correlation measure than MDL and relief algorithm due to its robustness to dataset size.

3.8 Chapter Conclusion

This chapter outlines the components of the characterization system proposed in this research. We used four datasets which contain the works of Van Gogh, Rembrandt, the Impressionists, and Cuno Amiet; each dataset is divided into patches in the size of 500x500 pixels. The datasets are selected according to their varying degree of similarity with Van Gogh. Before visible brushstrokes are segmented, the images in the datasets are converted into CIELAB colour space and filtered with MHN and circular filter. The filtering process is done to improve the result of visible brushstroke segmentation.

We proposed four methods for the extraction of visible brushstrokes: Iterative Extraction Method, Neutrosophy-based Segmentation Method, Texture

Boundary Detection Method, and Gabor Filter-based Segmentation Method. From the brushstroke regions obtained from those methods, we extracted shape and texture features for the classification. We did not consider colour in our feature extraction because of Van Gogh's unconventional use of colours throughout his career as an artist. The extracted features are then selected using CFS evaluation with the symmetrical uncertainty correlation metric. This feature selection process is essential to improve the features' ability to describe the classification model of each painter represented by them. It is also beneficial for improving the classification accuracy.

Chapter 4

The Classifications of Van Gogh's Brushtroke Features

4.1 Introduction

In machine learning, classification is a process of grouping instances of data together based on several characteristics. When the characteristics are predetermined, the classification is *supervised*. On the other hand, *unsupervised* classification is done when the characteristics are not predetermined. In this case, the classifier identifies common characteristics to group the data.

We do binary classifications of brush stroke features from the paintings of Van Gogh and the other three classes: Rembrandt, the Impressionists, and Cuno Amiet. We do not perform a multiclass classification since we are focusing on differentiating Van Gogh's brushstrokes features instead of other painters. The classification setup is similar to the one versus all classification. The classifications are done using the multilayer perceptron (MLP) and the open source Java implementation of C4.5 decision tree (J48) (Bhargava et al., 2013) (Chaudhuri and Bhattacharya, 2000) and are done in pairs: (VG, R), (VG, IMP), and (VG, CA). We also use 10-fold cross validation and 30/70

percentage split for evaluating the predictive performance of the classification model. The purpose of cross validation is to measure the ability of the classification model in performing while a new sample of dataset is used for testing and training.

4.2 Data Preprocessing

4.2.1 Dataset Balance Check

We used a total number of 41 high-resolution paintings which were divided into 1,264 patches of 500x500 pixels. The paintings were then divided into four groups with respect to their varying degree of similarity with the works of Van Gogh. Those four groups are VG, R, IMP, and CA. For the complete list of paintings and their details, please refer to Section 3.2.

A dataset is considered as a balanced dataset if it contains nearly equal number of observations for each class. Although in practice dataset imbalances are common, such as in detecting rare disease or credit card fraud, a balanced dataset is more desirable. This is because some classifiers, especially rule-based classifiers such as decision tree, are sensitive to the interclass proportions in the dataset. In the case of an imbalance dataset, additional instances can be generated to balance the interclass proportion with respect to the statistical properties of the original instances (Putri, Fanany, and Arymurthy, 2011).

We measure our dataset balance using Shannon entropy (Shannon, 2001). The measure of dataset balance with Shannon entropy is given as follows:

$$Balance = \frac{H}{logk} = \frac{-\sum_{i=1}^{k} \frac{c_i}{n} log \frac{c_i}{n}}{logk} \tag{4.1}$$

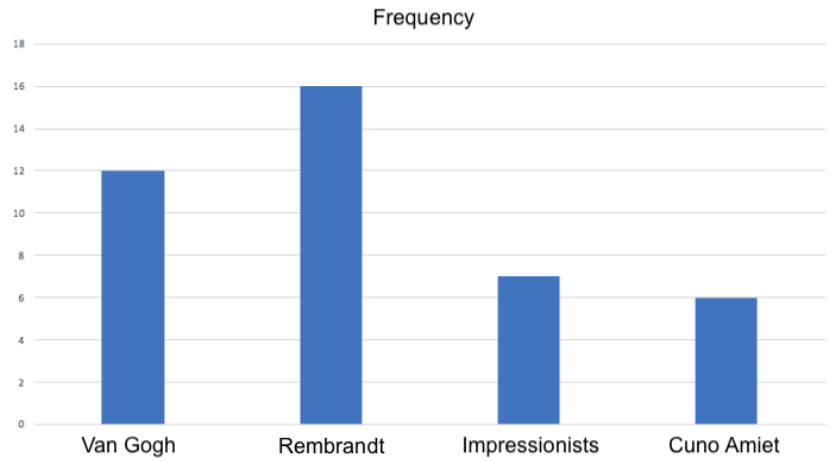

a

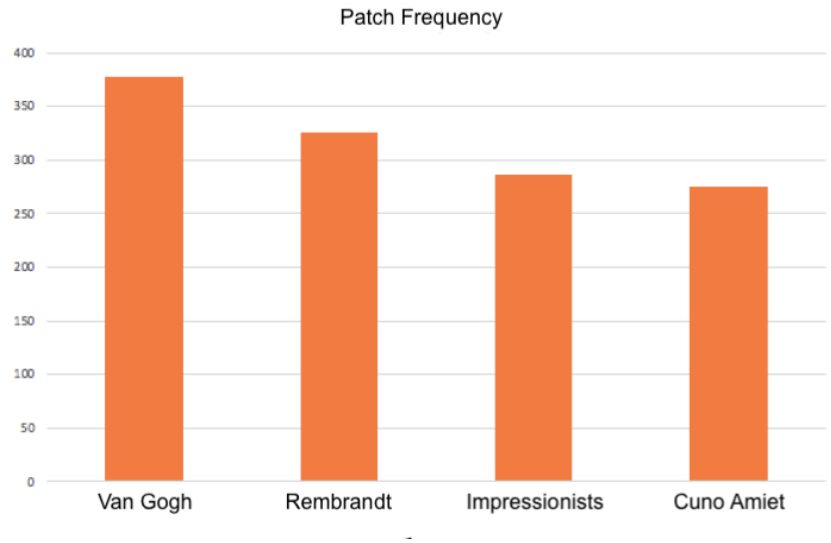

b

FIGURE 4.1: (a) The number of painting instances in every datasets, and (b) the number of patches in every datasets.

with c_i is the number of instances in class i, k is the number of different classes, and n is the total number of instances in the dataset.

The balance measures for each pair of datasets for binary classification are given in Table 4.1. As shown in the table, the balance measure for every pair is close to 1, which indicates that our dataset is already balanced and no further treatment should be conducted in order to address the imbalance.

TABLE 4.1: The Balance Measures of the Dataset Pair for Classification.

Dataset 1	Patches in Dataset 1	Dataset 2	Patches in Dataset 2	Balance Measure
VG	377	R	326	0.99620
VG	377	IMP	286	0.98637
VG	377	CA	275	0.98227

4.2.2 Outlier Removal

We remove outliers from our data to improve the classification result. This step is important, since we have the zero padded regions from the patch division which are not intended to be used for the classification. We use the *InterquartileRange* attribute filter in WEKA to detect outliers and extreme values using their interquartile range (IQR) values. IQR is a measure of statistical dispersion which measures the difference of the upper and lower quartile. In a sorted dataset, the upper quartile Q_3 is the middle value between the median and the maximum value. Meanwhile, the lower quartile Q_1 is the middle value between the minimum value and the median.

$$IQR = Q_3 - Q_1 \tag{4.2}$$

The process of outlier removal for each attribute in the dataset is given below:

1. Sort the atrribute's instances in ascending order.
2. Calculate the first quartile Q_1 and third quartile Q_3, then obtain the IQR.
3. Decide the outlier factor. In this research, we use 1.5 as the outlier factor.

4. Compute the boundary (b_1,b_2) with the following equations:

$$b_1 = Q_1 - (1,5 * IQR) \tag{4.3}$$

$$b_2 = Q_3 + (1,5 * IQR) \tag{4.4}$$

5. Filter out the data outside (b_1, b_2).

In WEKA, outlier removal process is given in the following steps:

1. Load the dataset into WEKA explorer. Click *Open file* and choose the dataset from its directory.
2. Under *Filter*, click *Choose* and select *unsupervised.attribute.InterquartileRange*. Click *Apply*.
3. Save the dataset by clicking *Save*.
4. Open the filtered dataset in Microsoft Excel. Notice that there are two extra columns called *Outlier* and *ExtremeValues*. Filter the instances using those columns.
5. Save the dataset which has the outliers and extreme values removed. This dataset is ready for normalization.

4.2.3 Data Normalization

Data normalization is a preprocessing step in machine learning when the values of an attribute are scaled to the range [0,1]. Data normalization is essential because it will remove bias and inaccuracy caused by an attribute that has a broad range of values, especially for measuring distances between instances. The aim of data normalization is to normalize the range of all attributes so that each attribute has the same influence over the dataset.

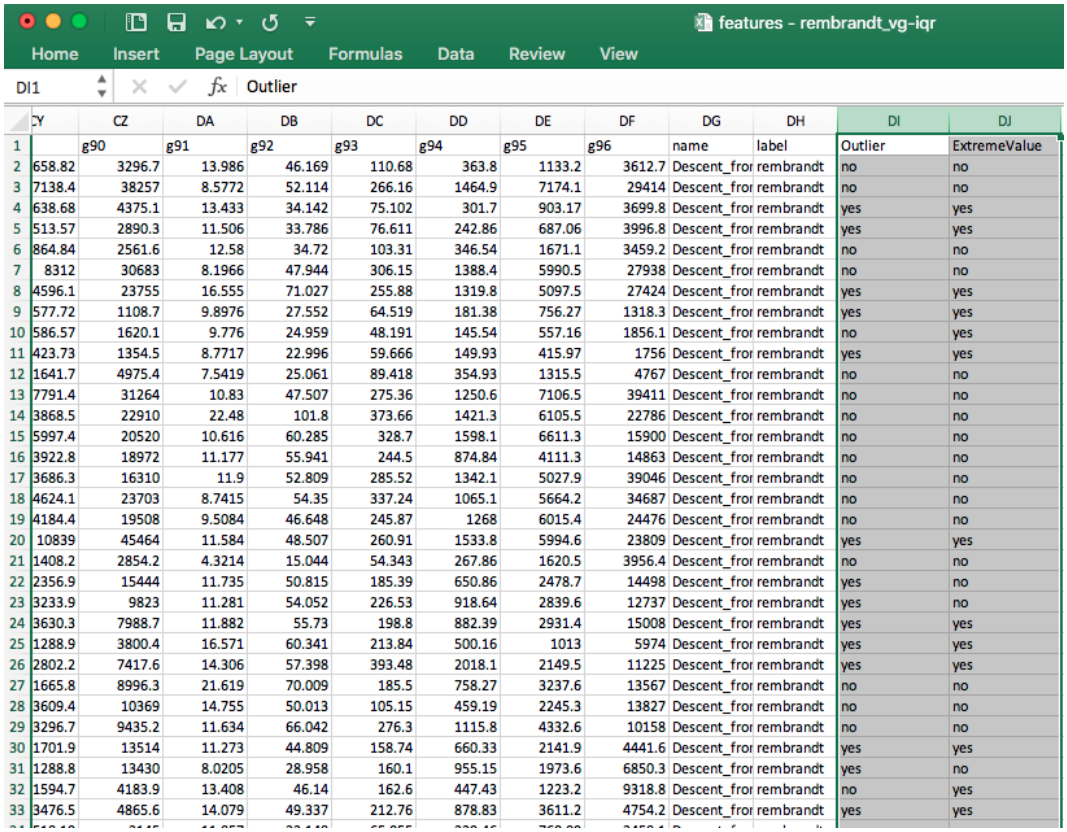

features - rembrandt_vg-iqr

Home Insert Page Layout Formulas Data Review View

DI1 Outlier

	CY	CZ	DA	DB	DC	DD	DE	DF	DG	DH	DI	DJ
1		g90	g91	g92	g93	g94	g95	g96	name	label	Outlier	ExtremeValue
2	658.82	3296.7	13.986	46.169	110.68	363.8	1133.2	3612.7	Descent_fro	rembrandt	no	no
3	7138.4	38257	8.5772	52.114	266.16	1464.9	7174.1	29414	Descent_fro	rembrandt	no	no
4	638.68	4375.1	13.433	34.142	75.102	301.7	903.17	3699.8	Descent_fro	rembrandt	yes	yes
5	513.57	2890.3	11.506	33.786	76.611	242.86	687.06	3996.8	Descent_fro	rembrandt	yes	yes
6	864.84	2561.6	12.58	34.72	103.31	346.54	1671.1	3459.2	Descent_fro	rembrandt	no	no
7	8312	30683	8.1966	47.944	306.15	1388.4	5990.5	27938	Descent_fro	rembrandt	no	no
8	4596.1	23755	16.555	71.027	255.88	1319.8	5097.5	27424	Descent_fro	rembrandt	yes	yes
9	577.72	1108.7	9.8976	27.552	64.519	181.38	756.27	1318.3	Descent_fro	rembrandt	yes	yes
10	586.57	1620.1	9.776	24.959	48.191	145.54	557.16	1856.1	Descent_fro	rembrandt	no	yes
11	423.73	1354.5	8.7717	22.996	59.666	149.93	415.97	1756	Descent_fro	rembrandt	yes	yes
12	1641.7	4975.4	7.5419	25.061	89.418	354.93	1315.5	4767	Descent_fro	rembrandt	no	no
13	7791.4	31264	10.83	47.507	275.36	1250.6	7106.5	39411	Descent_fro	rembrandt	no	no
14	3868.5	22910	22.48	101.8	373.66	1421.3	6105.5	22786	Descent_fro	rembrandt	no	no
15	5997.4	20520	10.616	60.285	328.7	1598.1	6611.3	15900	Descent_fro	rembrandt	no	no
16	3922.8	18972	11.177	55.941	244.5	874.84	4111.3	14863	Descent_fro	rembrandt	no	no
17	3686.3	16310	11.9	52.809	285.52	1342.1	5027.9	39046	Descent_fro	rembrandt	no	no
18	4624.1	23703	8.7415	54.35	337.24	1065.1	5664.2	34687	Descent_fro	rembrandt	no	no
19	4184.4	19508	9.5084	46.648	245.87	1268	6015.4	24476	Descent_fro	rembrandt	no	no
20	10839	45464	11.584	48.507	260.91	1533.8	5994.6	23809	Descent_fro	rembrandt	yes	yes
21	1408.2	2854.2	4.3214	15.044	54.343	267.86	1620.5	3956.4	Descent_fro	rembrandt	no	no
22	2356.9	15444	11.735	50.815	185.39	650.86	2478.7	14498	Descent_fro	rembrandt	yes	no
23	3233.9	9823	11.281	54.052	226.53	918.64	2839.6	12737	Descent_fro	rembrandt	yes	no
24	3630.3	7988.7	11.882	55.73	198.8	882.39	2931.4	15008	Descent_fro	rembrandt	yes	yes
25	1288.9	3800.4	16.571	60.341	213.84	500.16	1013	5974	Descent_fro	rembrandt	yes	yes
26	2802.2	7417.6	14.306	57.398	393.48	2018.1	2149.5	11225	Descent_fro	rembrandt	yes	yes
27	1665.8	8996.3	21.619	70.009	185.5	758.27	3237.6	13567	Descent_fro	rembrandt	no	no
28	3609.4	10369	14.755	50.013	105.15	459.19	2245.3	13827	Descent_fro	rembrandt	no	no
29	3296.7	9435.2	11.634	66.042	276.3	1115.8	4332.6	10158	Descent_fro	rembrandt	no	no
30	1701.9	13514	11.273	44.809	158.74	660.33	2141.9	4441.6	Descent_fro	rembrandt	yes	yes
31	1288.8	13430	8.0205	28.958	160.1	955.15	1973.6	6850.3	Descent_fro	rembrandt	yes	no
32	1594.7	4183.9	13.408	46.14	162.6	447.43	1223.2	9318.8	Descent_fro	rembrandt	no	yes
33	3476.5	4865.6	14.079	49.337	212.76	878.83	3611.2	4754.2	Descent_fro	rembrandt	yes	yes

For each value x in an attribute i, we use min-max normalization which is given in the formula below:

$$normalized(x_i) = \frac{x - \min(i)}{\max(i) - \min(i)} \tag{4.5}$$

In WEKA, the normalization is done in these following steps:

1. Load the dataset into WEKA explorer. Click *Open file* and choose the dataset from its directory.
2. Under *Filter*, click *Choose* and select *unsupervised.attribute.Normalize*.
3. Click *Apply* and *Save* to get the dataset with the normalized attribute
4. The dataset is ready for the classification.

4.3 Classification Process

4.3.1 Classifiers

We use Multilayer Perceptron (MLP) and C4.5 decision tree (J48) classifiers on WEKA to classify our datasets. The classifiers have been chosen since they are proven to be able to handle numerical data well with their own different approaches. Both MLP and J48 are known for their comprehensibility, which made them useful for the problem of painting style classification since it is a rule generation problem. They also have the ability to select features from the dataset with the utmost discrimination. The description for each classifiers are given below.

Multilayer Perceptron (MLP)

Multilayer Perceptron (MLP) is a feedforward artificial neural network. It contains several connected layers of nodes which are connected in a direct graph. This structure of nodes causes the input signal to not be able to go back to where it came from. Every node in the network (with the exception of input nodes) has a non-linear activation function. MLP classifies the instances using backpropagation algorithm (Werbos, 1990), which calculate the non-linear function between the input and the output by adjusting the internal weight values. The MLP configurations we used are given in Table 4.2.

TABLE 4.2: WEKA MLP Classifier Configurations

Parameters	Value
Option to autocreate the network connections	True
Option to allow learning rate decay	False
Learning rate for the backpropagation	0.3
Momentum rate for the backpropagation	0.2
Option to filter nominal to binary	True
Option to normalize attributes	True
Option to normalize numeric class	True
Number of epochs	500
Threshold for number of consecutive errors	20
Percentage of validation set	0
Value to seed the random number generator	0

J48 Decision Tree

In this research, we use the J48 algorithm, which is the open source Java implementation of C4.5 decision tree. C4.5 decision tree is the extension of Iterative Dichotomiser (ID3) (Quinlan, 1986). It uses the same principal as ID3 in building the decision trees from a set of training data using information gain (see Eq. 3.18). The additional features of C4.5 from ID3 include support for missing values, tree pruning, and derivation of rule (Kaur and Chhabra, 2014).

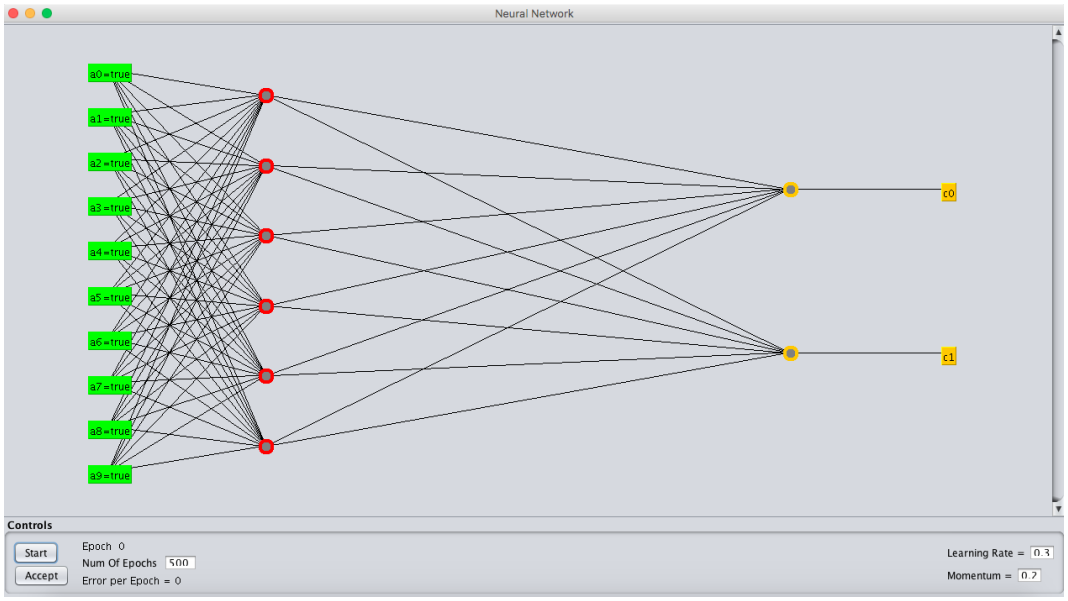

FIGURE 4.2: The example of MLP architecture in WEKA's *MultilayerPerceptron* GUI. The number of neurons are reduced for more readability.

TABLE 4.3: WEKA J48 Classifier Configurations

Parameters	Value
Binary splits	False
Option for collapsing the tree	True
Pruning confidence	0.25
Option for making split point actual value	False
Minimum number of instances	2
Number of folds for reduced error pruning	3
Option for reduced error pruning	False
Seed for random data shuffling	1
Option to perform subtree raising	True

C4.5 is a univariate decision tree which handles one attribute per test node. It selects the the attributes that best split the samples into the classes based on the normalized information gain. Once the attribute with the highest gain is chosen, the algorithm then evaluates the smaller sublists by recursion. This step is called as *branching*. When all the instances belong to the same class, the resulting tree will be a single leaf labelled with the class.

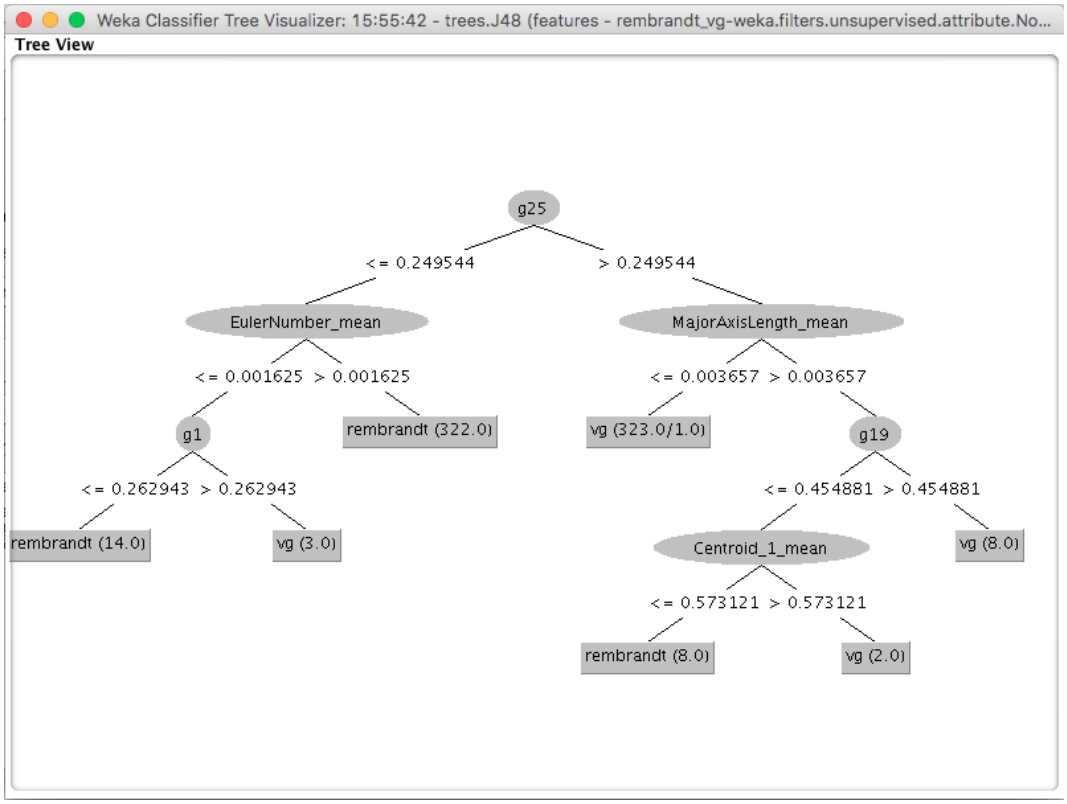

FIGURE 4.3: The example of decision tree generated using WEKA's J48 algorithm. The tree represents the classification between VG and R datasets.

4.3.2 Performance Measures

Classification Accuracy

In machine learning, the summary of the algorithm's performance can be shown using the *confusion matrix*. In binary classification, the confusion matrix is a table containing two rows for the instances in the actual classes and two columns for the instances in the predicted classes.

In Figure 4.4, the True Positive (TP) and True Negative (TN) consists of correctly classified instances. In contrast, the False Negative (FN) contains the positive instances which were incorrectly classified as negatives while the False Positive (FN) contains the negative instances which got incorrectly classified as positives. FP is also known as the Type 1 Error while FN is

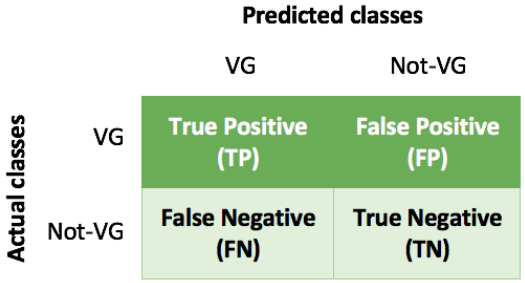

FIGURE 4.4: The Confusion Matrix

known as the Type 2 Error. When performing our classification, we treat VG as the positive dataset and the other datasets that is not VG as the negatives.

Classification accuracy is the most intuitive measure of performance that can be calculated based on the number of instances in the cells of confusion matrix. It can be obtained from the ratio of correct classifications made and the number of all classifications.

$$accuracy = \frac{TP + TN}{TP + TN + FP + FN} \tag{4.6}$$

Classification accuracy might be considered as the most straightforward metric to measure the performance of a machine learning model. However, a model with high classification accuracy is not guaranteed to have better predictive ability. A phenomenon called *The Accuracy Paradox* states that a model with a given classification accuracy may perform better than another model with a higher classification accuracy. Since we aim to proof that our features represents the characteristic of Van Gogh's brushstrokes, we desire a minimum number for instances in FP, which are the ones which belong to the other painter, but were classified as Van Gogh. In the case of a binary classification which emphasises the minimisation of the FP, including our classification, an additional metric must be introduced to accompany classification accuracy.

F-measure

The F-measure or F1 score is a performance measure which takes *precision* and *recall* into account. Precision is the ratio of TP and all positive results (TP and TN), and recall is the ratio of TP and all the instances in the positive class. F-measure is the harmonic average of precision and recall, and it has the range of [0,1]. The measure of precision corresponds to the model's ability to classify more instances correctly than incorrectly — that is, the proportion of the instances that really belong to VG from those which are classified as VG. The measure of recall corresponds to the model's ability to classify the correct instances as much as possible, that is, the proportion of correctly classified VG instances from all VG instances.

We use the F-measure and do not take into account the true negatives because we are only interested in how the VG dataset will be correctly classified. The equation of F-measure is given as follows:

$$F - measure = 2 * \frac{precision * recall}{precision + recall} \tag{4.7}$$

4.3.3 Robustness Measure

Robustness is defined as the ability to handle various test cases, especially the erroneous ones. We use k-fold cross validation to measure the robustness of our model. In k-fold cross validation, the original sample is randomly partitioned into k equal sized subsamples. Of the k subsamples, a single subsample is retained as the validation data for testing the model, and the remaining $(k-1)$ subsamples are used as training data. The cross validation process is then repeated k times, with each of the k subsamples used exactly once as the validation data. The k results can then be averaged to produce a single estimation. The advantage of this method over repeated random

sub-sampling (see below) is that all observations are used for both training and validation, and each observation is used for validation exactly once. 10-fold cross-validation is commonly used, but in general k remains an unfixed parameter.

We use the stratified version of k-fold cross validation with $k = 10$. In stratified k-fold cross validation, the folds are selected so that the mean response value is approximately equal in all the folds. In the case of binary classification, this means that each fold contains roughly the same proportions of the two types of class labels.

4.3.4 Chapter Conclusion

This chapter elaborates the details of the binary classifications done in this work. Before we perform the classifications, we preprocess the datasets by checking their balance, removing outliers and extreme values, and normalizing them. We use MLP and J48 in WEKA to classify the datasets. The classifications are done in pairs between VG and the other three datasets: R, IMP, and CA. We then measure the performance of the models using the classification accuracy and f-measure. In addition, we also measure the robustness of the models by doing stratified 10-fold cross validation to ensure that the models can handle various test cases.

Chapter 5

Results and Discussion

5.1 Brushstroke Segmentation Results

5.1.1 Iterative Extraction Method

In this method, the adaptive scaling of blobs within a brush region can cause a smaller blob to be detected within a larger blob as shown in Figure 5.1, resulting in "lumps" and thick lines in the detected brushstroke's skeleton. Such artefacts can be easily removed by using another set of flags for pixels within the detected blobs in the current brush region.

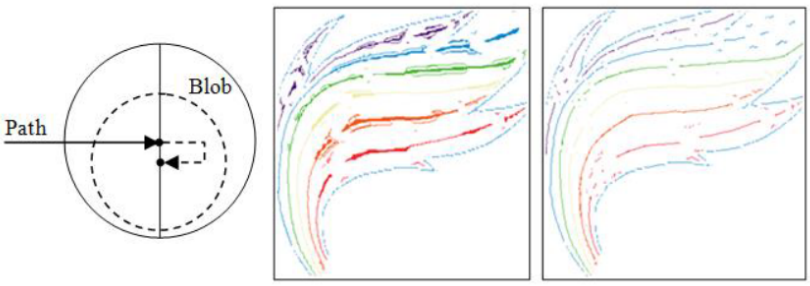

FIGURE 5.1: The removal of thick lines in the skeleton of detected brushstrokes

The brush radii used along the 8 directions at the current position (Figure 3.8) have integral values, and it is quite likely that we will get more than one direction with the same value for maximum radius. In such cases, we

can assign a directional priority to indicate the preferred brushstroke path. For example, a left to right horizontal brushstroke can be given priority if that direction is among others that gave the maximum radius. A slight variation of lightness value can often be seen across a brushstroke's region. The method shown in Figure 3.8. uses the colour value at P_0 as the reference for the entire region. We could modify this approach by using the average of matched colour values within the current blob position as the reference for the next iteration, i.e., for the blobs searched along the 8 neighbouring directions. Such a variation of reference colour produces longer continuous paths instead of several broken segments.

When the blob radius reduces to a small value (for instance lower than 5 pixels), we require larger thresholds to accommodate extraneous pixels that do not have a colour that matches with the reference colour. For example, when the radius is less than 10, a 10% threshold for extra pixels would give a value 0. Moreover at a small radius value, we get only a very coarse approximation of a circular shape. In general, regions corresponding to very thin brushstrokes must be treated separately. Several such regions commonly appear in between larger segments of uniform colour. We use 3x3 and 5x5 square regions called "windows" to render small fragmented segments in the input image. The method of filling windows is distinctly different from that of blobs. Windows do not form a brush path; in other words, a window does not have any "connected" windows. Secondly there is no reference colour for a window. A window is filled using a maximum voting method that determines the most commonly occurring colour value in that small segment. Thirdly, the size of the window can vary based on the frequency of occurrence of a colour value in that region.

In Figure 5.2, a small region around a set of previously visited pixels is shown. The visited pixels are indicated in red colour, and the clear pixel

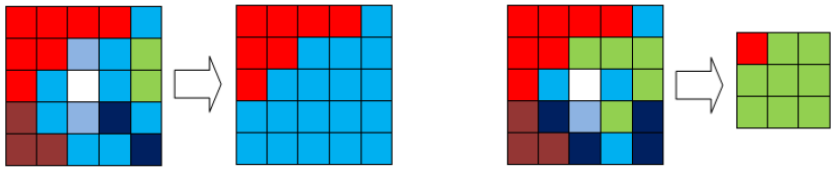

FIGURE 5.2: The construction of a 5x5 window and a 3x3 window.

is the current location (P_0) of the window. In Figure 5.2 (left), there are 8 pixels of cyan colour in the 5x5 neighbourhood. The maximum frequency (or vote) of colours in the neighbourhood determines the size of the window. Since we used 8 as the threshold, the colour cyan is used to fill the unvisited pixels in the 5x5 neighbourhood. The second example in Figure 5.2 (right) shows the colour green having a maximum vote of 5. In this case we use a 3x3 window.

There are similarities in both approaches and outputs between algorithms for the extraction of edges and brush skeletons. An edge detection algorithm looks for gradients across regions while a brush skeleton represents a direction of homogeneity in colour values. A brush skeleton can be considered as a line (or multiple lines) between parallel edges of a region of nearly uniform colour. Both algorithms aim to provide outputs consisting of fewer fragmented lines, and this is achieved by pre-processing the image to get rid of high frequency components, and by careful selection of colour thresholds (see Equation 3.4).

There are mainly two reasons for the discontinuities in the skeleton images shown in Figure 5.3. The iterative nature of the algorithm causes regions corresponding to large blob radius to be detected first, and smaller adjoining sections will be detected only in subsequent skeletons. Since a skeleton always starts from the centre of a blob, there will be some gap between the two skeletons even if the two regions meet at a point. Secondly, there will be small intervening pixels with colour values outside the threshold required

FIGURE 5.3: The skeleton of brush regions extracted by the iterative extraction method (Putri and Mukundan, 2015). We used photographs to test and benchmark our algorithm in extracting homogenous regions using their skeleton.

for matching with the reference colour, causing a skeleton to terminate and a new skeleton to begin after a few pixels. Increasing the threshold, on the other hand causes large blob regions to appear in the output. With a tighter threshold, only few blobs of large radius are seen (e.g., the stern of the boat in Figure 5.3). The sky image has large regions of nearly constant illumination and therefore results in longer skeletons with large blob radius. The effect of assigning directional priority to horizontal can be clearly seen in the path image, since otherwise skeletons could be in any arbitrary direction. The number of discontinuities along skeletons could be reduced using adaptive variations in the colour threshold for the blobs along the skeleton.

Figure 5.4 shows the brushstroke regions that had been rendered back based on their skeletons. Although the implementation of this method is straightforward, the result is not very satisfactory. This is because in the re-rendering

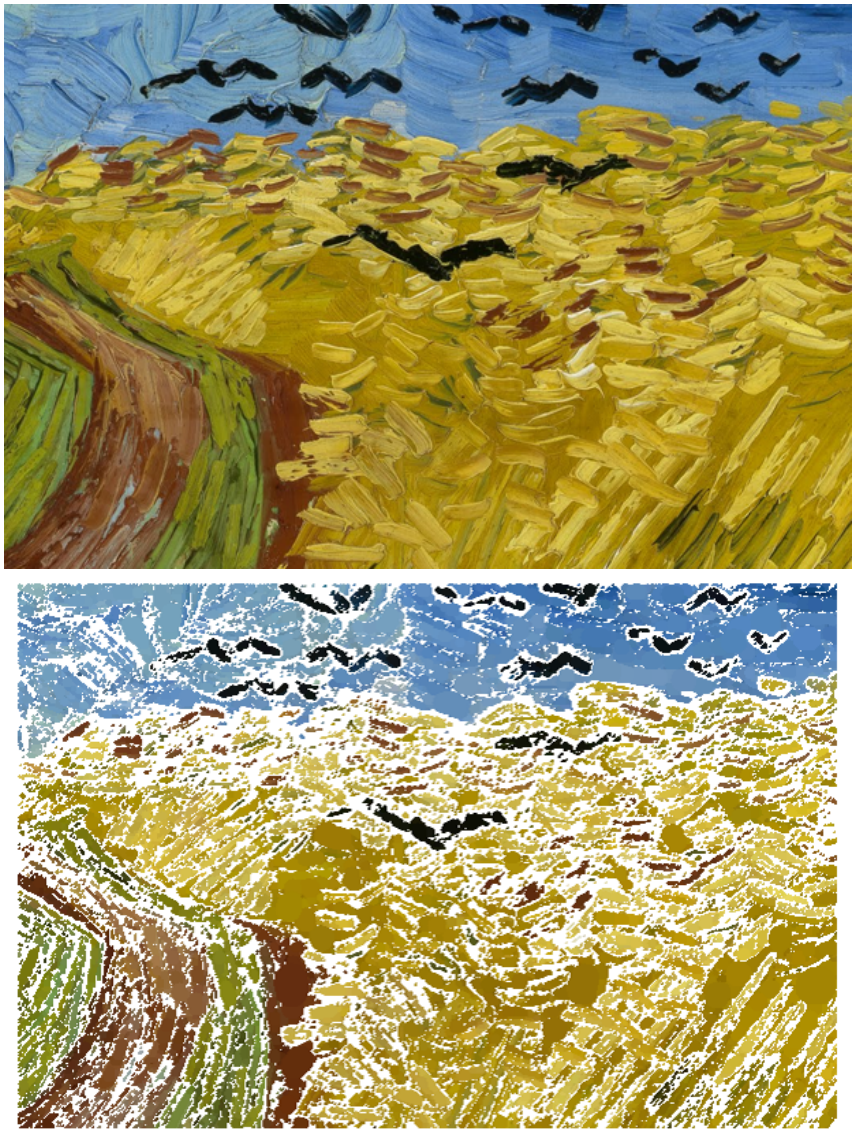

FIGURE 5.4: The result of iterative extraction in Van Gogh's *Wheatfield with Crows*

process, the overall brushstroke shapes are redrawn using the blob movement with adaptive scaling. The result of this action is the elimination of several pieces of information that might be useful in characterizing the brushstrokes.

5.1.2 Texture Boundary Detection Method

Texture boundary detection identifies the local entropy value from every pixels in the input image. The entropy value is calculated from the 9x9

neighbourhood of every pixel. A pixel that belongs to the same region has similar entropy to its neighbours because a brushstroke region has a uniform texture of its own. The transition between the brushstroke region and non-brushstroke region can be detected by the change of entropy between the pixels in those regions.

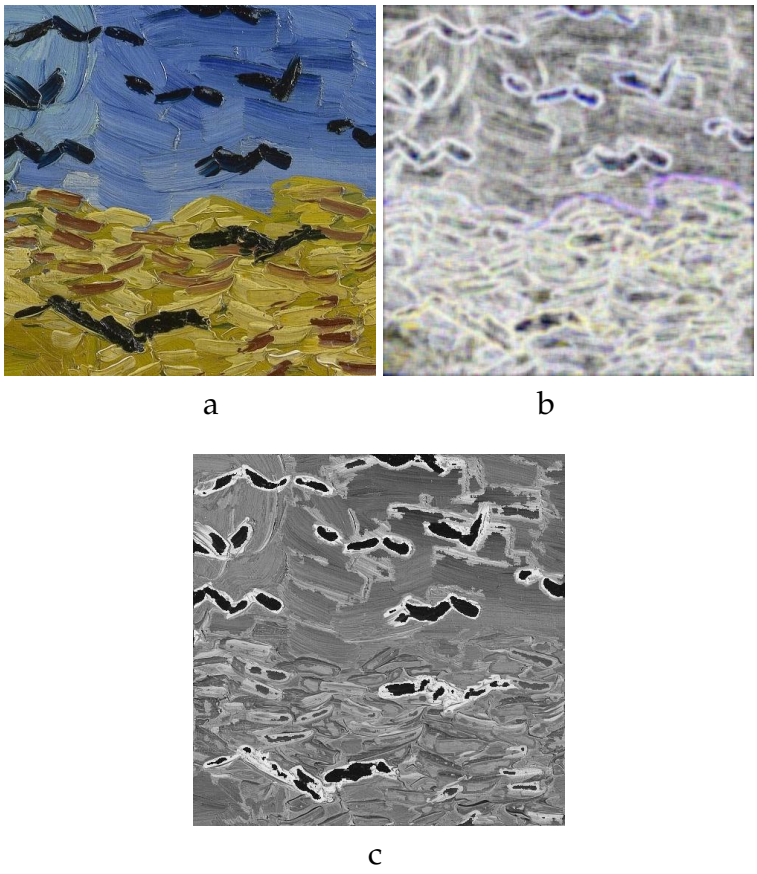

FIGURE 5.5: (a) The original image, (b) the entropy filtered of (a), and (c) the visible brushstroke regions (in dark grey) based on the DBSCAN clustering result of the values in (b).

The entropy value is mapped into the range of [0, 255] in order to visualize the groupings of the pixels with similar entropy. In Figure 5.5, it can be seen that the pixels that belong to the same region, for instance the crows, have similar entropy. This method is able to yield a satisfactory result in detecting the visible brushstrokes. However, the segmentation result is dependent on the clustering mechanism that is used. In this work, we used DBSCAN clustering to obtain the area with the visible brushstrokes since it computes

the clusters based on the density of the pixels with similar entropy value. It is possible to achieve a more precise result on detecting visible brushstrokes area using an extended version of DBSCAN algorithm, for instance, the work of Kisilevich, Mansmann, and Keim (2010).

5.1.3 Gabor Filter Based Segmentation Method

In this method, we use magnitude response as suggested by Clausi and Jernigan (2000) as supposed to real response to capture the features of the images with the filter bank. The reason for this is that the real components are not able to represent the full response of the filter, thus will result in a noisy segmentation and more innacurate clustering.

The convoluted image of the magnitude response from all filters in the filter bank is given in Figure 5.6.

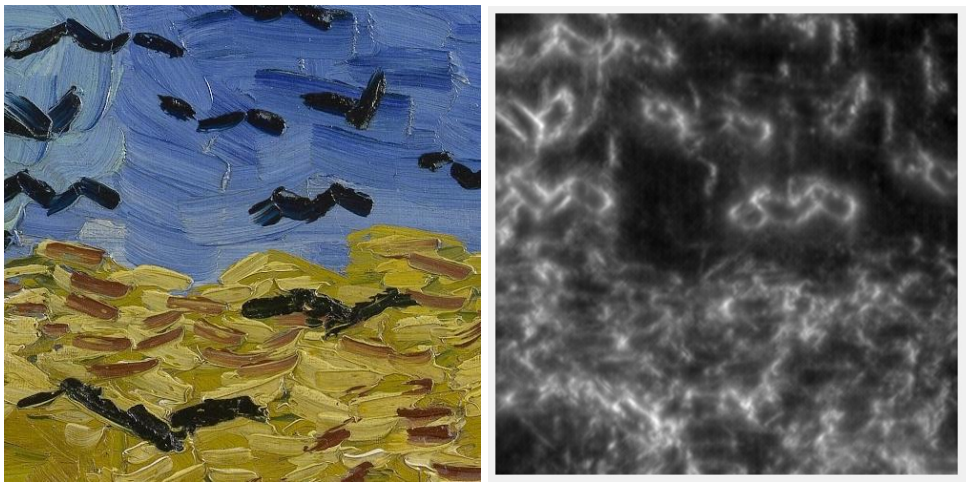

FIGURE 5.6: The original image with its Gabor convoluted counterpart from the Gabor magnitude response of all the gabor filters in the filter bank.

From Figure 5.6, it can be seen that the method can outline the visible brushstroke clearly, especially in the area of the crows with the blue sky background in which intensity level varies greatly between regions. It can also present the ochre background brushstrokes at the bottom of the image quite

visibly. Although those brushstrokes are visible enough when they are observed by our naked eyes, their segmentation with the Gabor filter is more complex since many of them are overlapping and blended with the other brushstrokes.

The region clustering result is given in Figure 5.7. We use DBSCAN algorithm to cluster the magnitude responses from the filter bank. The magnitude responses are stored in the form of a feature vector. Each dimension of the vector corresponds to different pairs of spatial-frequency (scale) and orientation. The magnitude responses represent the key texture information in every pixel in the image through different channels.

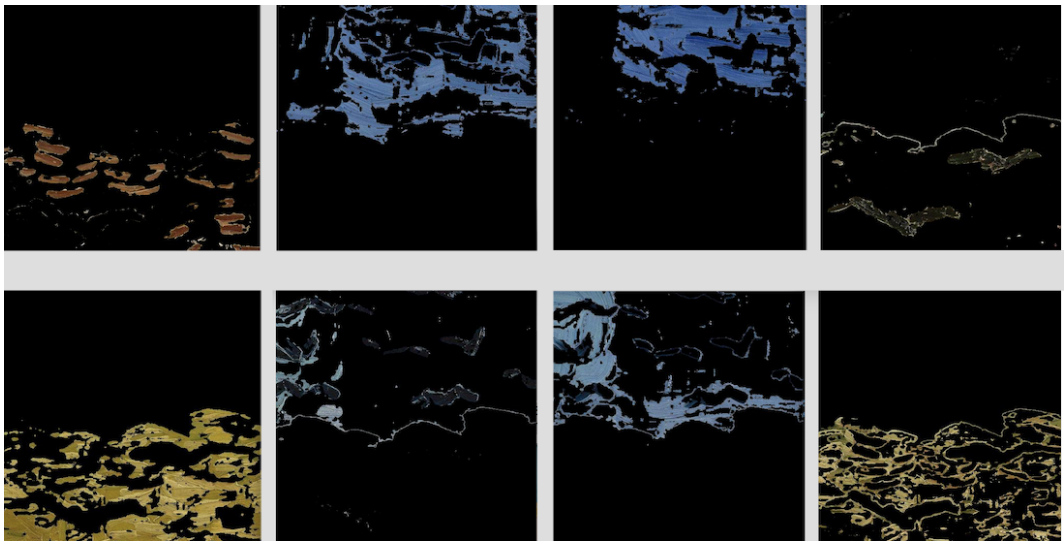

FIGURE 5.7: The clustering result of the pixels based on their Gabor magnitude response of $\lambda_i, i = (1, ..., 6) * \sqrt{2}$ and $\theta_j = \frac{j\pi}{8}, j = 0, ..., 7$.

DBSCAN clustered the magnitude responses into 8 different clusters that can be seen on Figure 5.7. The image appeared to be clustered based on the colours, but the clustering is indeed done by grouping similar magnitude response between pixels. Similar texture in several regions can be seen in paintings is due to the reason that the painter rendered those regions using the same brush size or did multiple rendering at the same time.

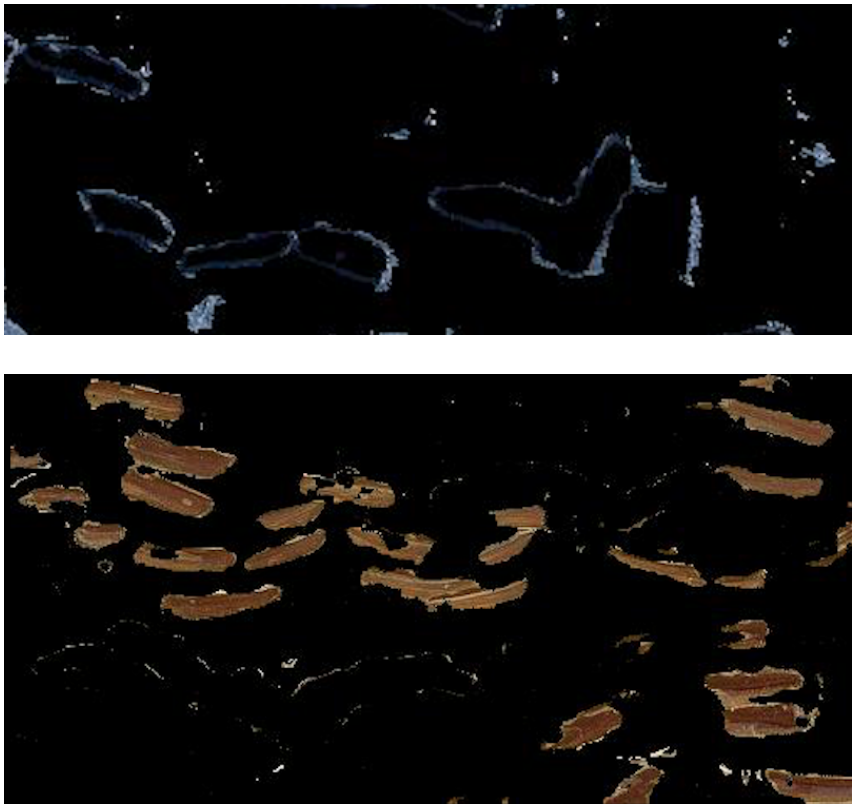

FIGURE 5.8: The visible brushstrokes extracted by the Gabor filter: the crows (top) and the brown accent of the wheatfield (bottom).

In Figure 5.7, it is visible that the cleanest visible brushstroke we obtained is the brown brushstrokes (top-left figure in Figure 5.7). The most recognizable brushstrokes, which are the crows are also got detected by this method.

5.1.4 Neutrosophy Based Segmentation Method

The results of our segmentation can be seen in Figure 5.10. The application of the circular filter before converting the image to neutrosophic domain significantly affects the outcome. Circular filtering has successfully magnified elliptical shapes of Van Gogh's brushstrokes. It has also removed noise and unnecessary details, such as streaks inside the stroke and concealed strokes which lies behind the visible strokes. While used together, circular filtering and neutrosophy based segmentation can complement each other in terms

a

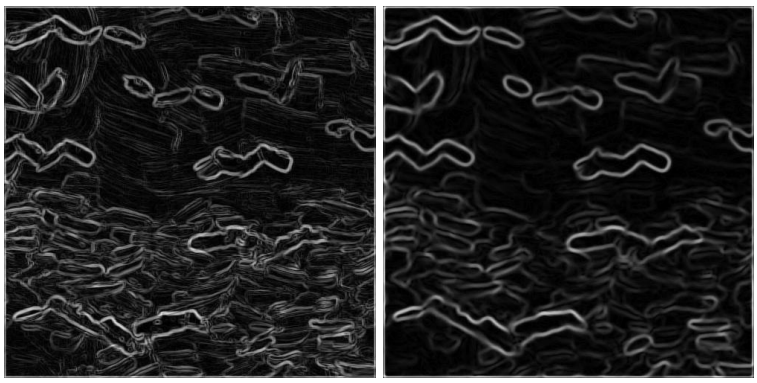

b c

FIGURE 5.9: (a) Original image, (b) the true domain of (a) without circular filtering, (c) the true domain of (a) with circular filtering.

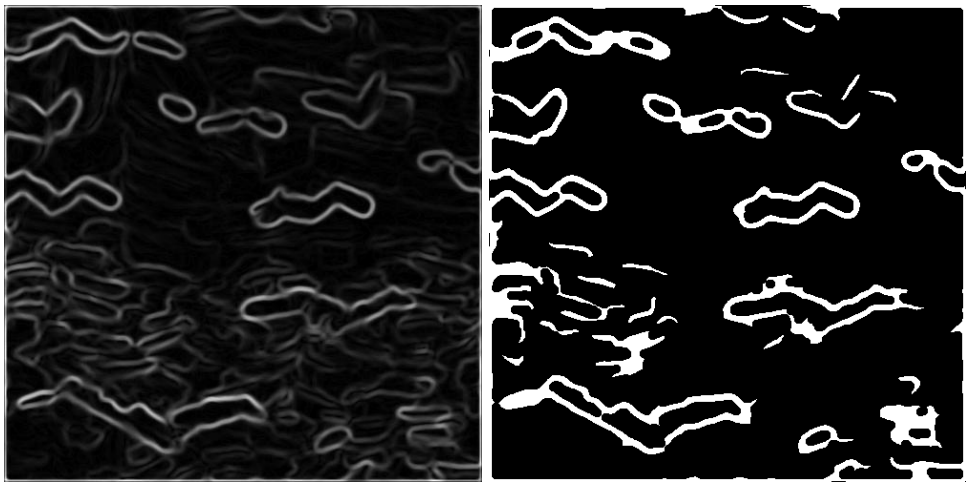

a b

FIGURE 5.10: (a) The true domain of the image (with circular filter), and (b) the thresholded and linked brushstrokes from (a).

of improving the segmentation result. Figure 5.9 gives a clear comparison of the effect of applying and not applying circular filter. As seen in Figure 5.9(c), the concealed and blended brushstrokes have been filtered out by circular filter, leaving a cleaner, more defined visible brushstroke edges.

5.2 Classification Results

5.2.1 Determining Van Gogh from Other Painters

In the binary classifications between the features extracted from VG and the other three datasets using the iterative extraction method, it is shown that the method does not produce representative features for the classification. In differentiating the instances in VG and R, which consist of the most obviously different instances from each other, the models misclassified around 20% of the instances. The classification result between VG and IMP is even poorer, given the average F-measure of 0.75 for both classifiers. This result may have been due to the ridges caused by the adaptive blob rescaling when the method tried to reconstruct the shape of the brushstroke after its skeleton is detected. Table 5.1 gives the classification results between the features of VG and the two datasets R and IMP extracted by the iterative extraction method.

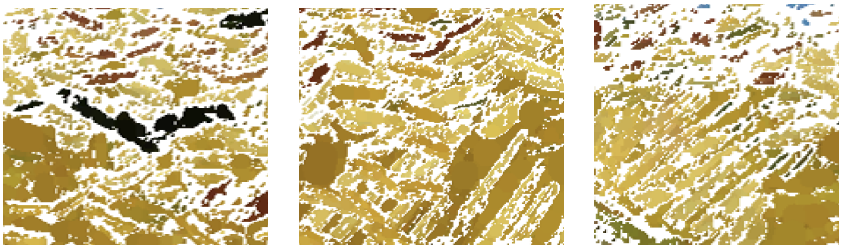

FIGURE 5.11: The ridges in the detected brushstrokes as the result of the adaptive blob scaling.

TABLE 5.1: The classification results of VG and the two datasets R and IMP by the iterative extraction method

Classes	Classifier	Testing Mode	Accuracy	F-Measure
VG & R	MLP	10-fold CV	80.52%	0.826
VG & R	MLP	30/70	81.53%	0.818
VG & R	J48	10-fold CV	78.32%	0.781
VG & R	J48	30/70	78.11%	0.786
VG & IMP	MLP	10-fold CV	74.74%	0.749
VG & IMP	MLP	30/70	75.03%	0.751
VG & IMP	J48	10-fold CV	73.22%	0.737
VG & IMP	J48	30/70	74.10%	0.745

The classification of brushstroke features extracted by the texture boundary detection and the Gabor filter based segmentation method yields similar results. This is because both methods have the same aim, which is to characterize the texture inside the visible brushstrokes. However, Gabor filter based segmentation performs better in differentiating VG and IMP. Since the instances in both VG and IMP have similar properties because the Post-Impressionist Van Gogh were influenced by the works of his Impressionist predecessors (Rubin, 1999), the two-dimensional entropy filter in the texture boundary method will give similar entropy values for both datasets. In contrast, the scale-invariant Gabor filter are able to extract some additional information that cannot be extracted by the texture boundary method, which are all processed in the signal domain. The classification results from those two methods are given in Table 5.2 and 5.3.

TABLE 5.2: The classification results of VG and the two datasets R and IMP by the texture boundary detection method

Classes	Classifier	Testing Mode	Accuracy	F-Measure
VG & R	MLP	10-fold CV	95.29%	0.953
VG & R	MLP	30/70	96.31%	0.963
VG & R	J48	10-fold CV	95.29%	0.953
VG & R	J48	30/70	95.85%	0.958
VG & IMP	MLP	10-fold CV	86.43%	0.864
VG & IMP	MLP	30/70	86.93%	0.869
VG & IMP	J48	10-fold CV	85.37%	0.853
VG & IMP	J48	30/70	90.95%	0.91

TABLE 5.3: The classification results of VG and the two datasets R and IMP by the Gabor filter based segmentation method

Classes	Classifier	Testing Mode	Accuracy	F-Measure
VG & R	MLP	10-fold CV	99.12%	0.991
VG & R	MLP	30/70	98.10%	0.981
VG & R	J48	10-fold CV	97.65%	0.976
VG & R	J48	30/70	97.14%	0.971
VG & IMP	MLP	10-fold CV	98.12%	0.981
VG & IMP	MLP	30/70	97.52%	0.975
VG & IMP	J48	10-fold CV	85.31%	0.852
VG & IMP	J48	30/70	86.34%	0.862

The neutrosophy based segmentation result is generally better than the Gabor filter based segmentation in differentiating the works of Van Gogh with Rembrandt and the Impressionists. However, it Computationally, the neutrosophy based segmentation is less expensive than the laborious Gabor filter based segmentation, which is done by first constructing a filter bank of multiple scales and orientations. The neutrosophy based segmentation gives a linear computational cost due to its linear fashion of calculating the membership values T, I and F of each pixels. The classification result of this method is given in the following Table 5.4.

TABLE 5.4: The classification results of VG and the two datasets R and IMP by neutrosophy based segmentation method

Classes	Classifier	Testing Mode	Accuracy	F-Measure
VG & R	MLP	10-fold CV	99.56%	0.996
VG & R	MLP	30/70	99.53%	0.995
VG & R	J48	10-fold CV	97.79%	0.978
VG & R	J48	30/70	98.57%	0.986
VG & IMP	MLP	10-fold CV	97.74%	0.977
VG & IMP	MLP	30/70	98.76%	0.988
VG & IMP	J48	10-fold CV	87.57%	0.876
VG & IMP	J48	30/70	87.58%	0.875

a b

FIGURE 5.12: *The Painting of Two Children* by Cuno Amiet (a) and Van Gogh (b) with their respected patch area along the chest of the girl on the right. Eventhough they are visually similar, the mean Euclidean distance of the brushstrokes in those two patches yield a result of $4.015x10^8$.

5.2.2 Determining Van Gogh from His Contemporary

Based on the classification result, the extracted brushstrokes and their feature are sufficient to distinguish Van Gogh from his contemporary. The system is also able to distinguish a painting that is a study of another painting. The two paintings in Figure 5.12 are the example of such paintings. The patches from both paintings are classified into their own painters which are Cuno Amiet and Van Gogh, respectively.

As seen in the previous results in classifying VG from R and IMP, the results in classifying VG and CA are similar between the texture boundary

TABLE 5.5: The classification results of VG and CA by the texture boundary detection method

Classes	Classifier	Testing Mode	Accuracy	F-Measure
VG & CA	MLP	10-fold CV	97.24%	0.972
VG & CA	MLP	30/70	98.46%	0.985
VG & CA	J48	10-fold CV	97.08%	0.971
VG & CA	J48	30/70	96.42%	0.964

TABLE 5.6: The classification results of VG and CA by the Gabor filter based segmentation method

Classes	Classifier	Testing Mode	Accuracy	F-Measure
VG & CA	MLP	10-fold CV	97.87%	0.973
VG & CA	MLP	30/70	98.31%	0.981
VG & CA	J48	10-fold CV	97.32%	0.969
VG & CA	J48	30/70	98.13%	0.989

detection method and Gabor filter based segmentation method. Both methods are equally good to differentiate the works of VG and CA which looks similar under a manual inspection, but have different texture due to Cuno Amiet's individual technique of brushstroke placement.

TABLE 5.7: The classification results of VG and CA by the iterative extraction method

Classes	Classifier	Testing Mode	Accuracy	F-Measure
VG & CA	MLP	10-fold CV	70.34%	0.708
VG & CA	MLP	30/70	71.77%	0.712
VG & CA	J48	10-fold CV	70.22%	0.704
VG & CA	J48	30/70	70.19%	0.707

TABLE 5.8: The classification results of VG and CA by neutrosophy based segmentation method

Classes	Classifier	Testing Mode	Accuracy	F-Measure
VG & CA	MLP	10-fold CV	89.34%	0.893
VG & CA	MLP	30/70	89.53%	0.895
VG & CA	J48	10-fold CV	88.03%	0.880
VG & CA	J48	30/70	85.62%	0.856

The neutrosophy based segmentation method, which succeeded previously in classifying VG from R and IMP is still giving good results though less than texture boundary detection and Gabor-filter based segmentation.

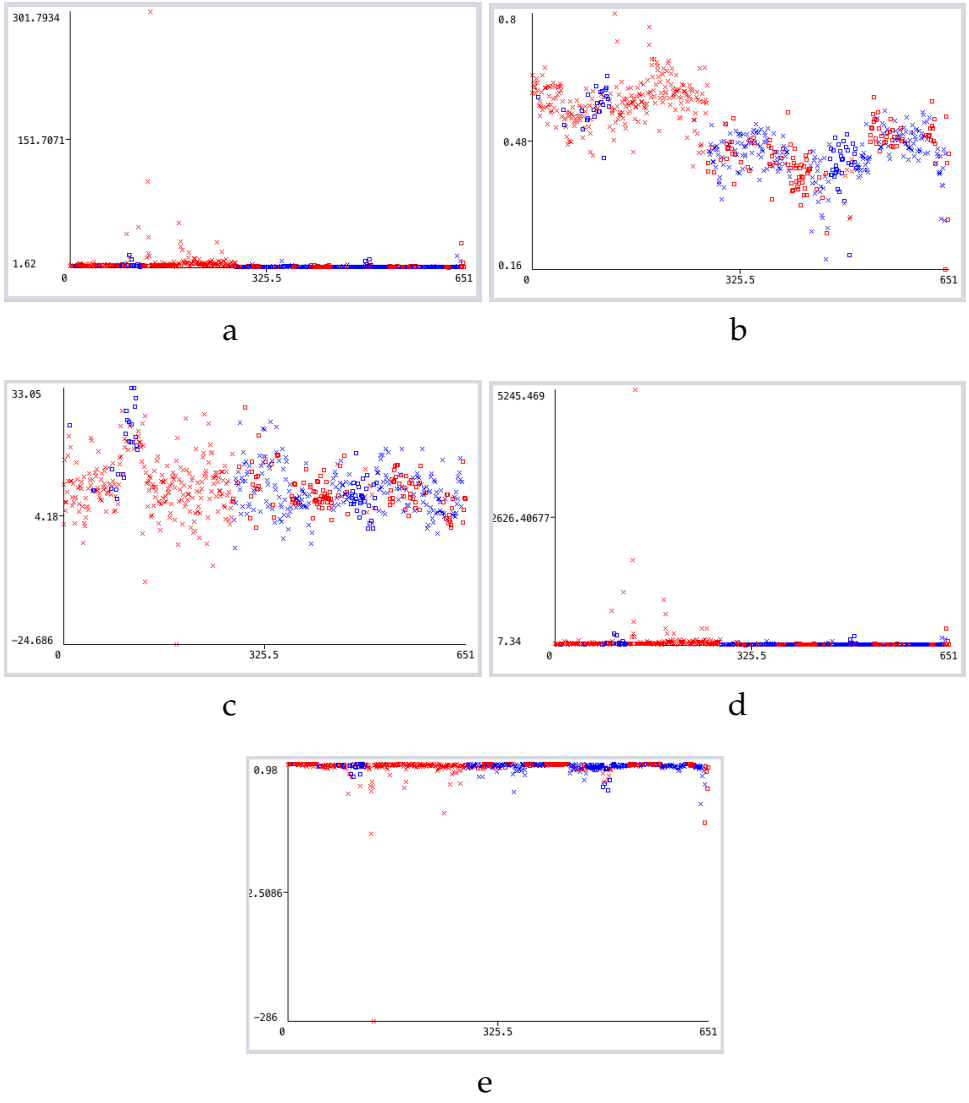

FIGURE 5.13: The visualization of separability of the shape features (a) major axis, (b) minor axis, (c) eccentricity, (d) Euler number, and (e) orientation from VG (blue) and CA (red).

We visualize of the separability of the brushstroke features obtained from the neutrosophy-based segmentation using K-means clustering with Euclidean distance. As mentioned earlier, Cuno Amiet's brushstrokes, although visually similar to Van Gogh's, have different textures. The physical similarity between the brushstrokes in both datasets can be visualized in Figure 5.13. It can be seen in Figure 5.13 that the shape features from the brushstrokes of Van Gogh and Cuno Amiet cannot be distinguished from one another. It is shown that the clusters of Van Gogh (blue) and Cuno Amiet (red) are

not separable, meaning that shape features are less useful for describing the brushstrokes of both group.

In contrast, the texture features obtained from Gabor magnitude response within the brushstrokes represent the instances from both datasets well. As seen in Figure 5.14, there are very few misclassified instances from both classes. In addition, the cluster separability between the two classes is clear enough.

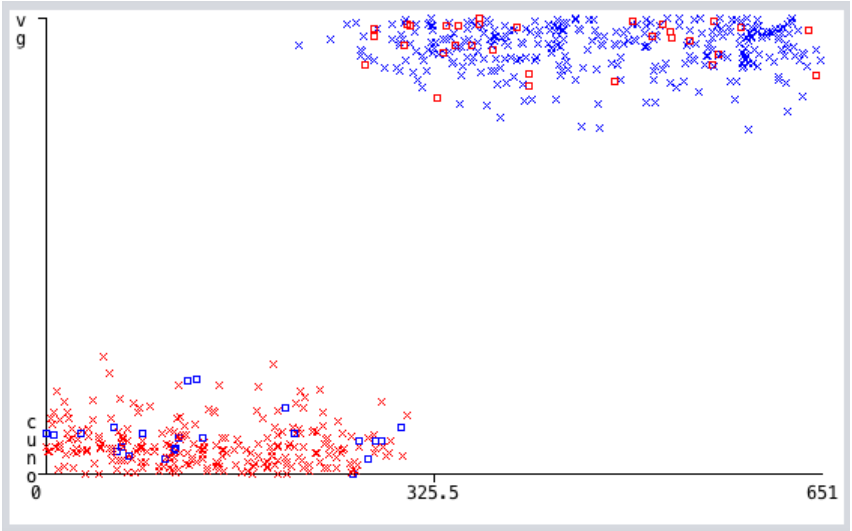

FIGURE 5.14: The visualization of cluster separability for the texture features of VG (blue) and CA(red).

5.3 Combining Brushstroke Features

Based on the experiment results, we combined the features from the regions extracted by the two methods that give the best classification result: Gabor filter based segmentation and neutrosophy based segmentation. Each of those methods represents both of the texture-based approach and edge-based approach of the brushstroke segmentation.

We performed similar classification setup with the previous experiments, which are by MLP and J48 with 30/70 training split and 10-fold cross validation. We also did feature selection with CFS evaluation before the classification. From our experiment, the texture features from both methods are shown to be dependent with each other. This leads to the texture features from neutrosophy based segmentation got filtered out by the CFS evaluation. This event is expected since both of the segmentation methods will have the same texture since the input images are the same. The significant difference between those methods are in the shape features, since both of them give different segmented brushstroke regions.

TABLE 5.9: The classification results of VG and the three datasets R, IMP, and CA by Gabor filter based and neutrosophy based segmentation method

Classes	Classifier	Testing Mode	Accuracy	F-Measure
VG & R	MLP	10-fold CV	97.94%	0.979
VG & R	MLP	30/70	98.10%	0.981
VG & R	J48	10-fold CV	98.38%	0.984
VG & R	J48	30/70	98.57%	0.986
VG & IMP	MLP	10-fold CV	94.92%	0.949
VG & IMP	MLP	30/70	92.55%	0.925
VG & IMP	J48	10-fold CV	88.14%	0.882
VG & IMP	J48	30/70	82.61%	0.826
VG & CA	MLP	10-fold CV	98.34%	0.983
VG & CA	MLP	30/70	98.55%	0.985
VG & CA	J48	10-fold CV	98.03%	0.980
VG & CA	J48	30/70	95.63%	0.956

In Table 5.10, it is shown that the combination of brushstroke features from Gabor filter based and neutrosophy based segmentation leads to the significant increase of performance in differentiating instances between VG and CA. The additional shape features from the Gabor filter based image segmentation give additional meaningful information to describe the instances in both classes, resulting in the increase of classification performances. It can be seen from Table 5.10 that the classification accuracy and F-measure

achieved using the features from neutrosophy based segmentation significantly increased by 10% on average after additional features from gabor filter based segmentation are introduced.

TABLE 5.10: The classification results of VG and the three datasets R, IMP, and CA by Gabor filter based and neutrosophy based segmentation method

Class.	Mode	Gabor Acc.	Gabor F-M	Neut. Acc.	Neut. F-M	Comb. Acc.	Comb. F-M
MLP	10-fold CV	97.87%	0.973	89.34%	0.893	98.34%	0.983
MLP	30/70	98.31%	0.981	89.53%	0.895	98.55%	0.985
J48	10-fold CV	97.32%	0.969	88.03%	0.880	98.03%	0.980
J48	30/70	98.13%	0.989	85.62%	0.856	95.63%	0.956

5.4 Chapter Summary

Based on the experiment results, the texture-based segmentation methods, which are the texture boundary detection method and Gabor-filter segmentation method, give satisfactory results in extracting visible brushstrokes that would yield representative features for the classification. Neutrosophy based segmentation method, which is an edge-based method performs better than any other methods, except for generating features for the classification of Van Gogh and Cuno Amiet. The iterative extraction method still performed reasonably well despite its simplicity with less than 20% of misclassified instances.

Combining features from Gabor filter based and neutrosophy based segmentation methods result in an increase of classification performance in classifying VG and CA. This is because the Gabor filter based segmentation provides additional useful information to describe the instances of both classes, which are additional Gabor-obtained shape features.

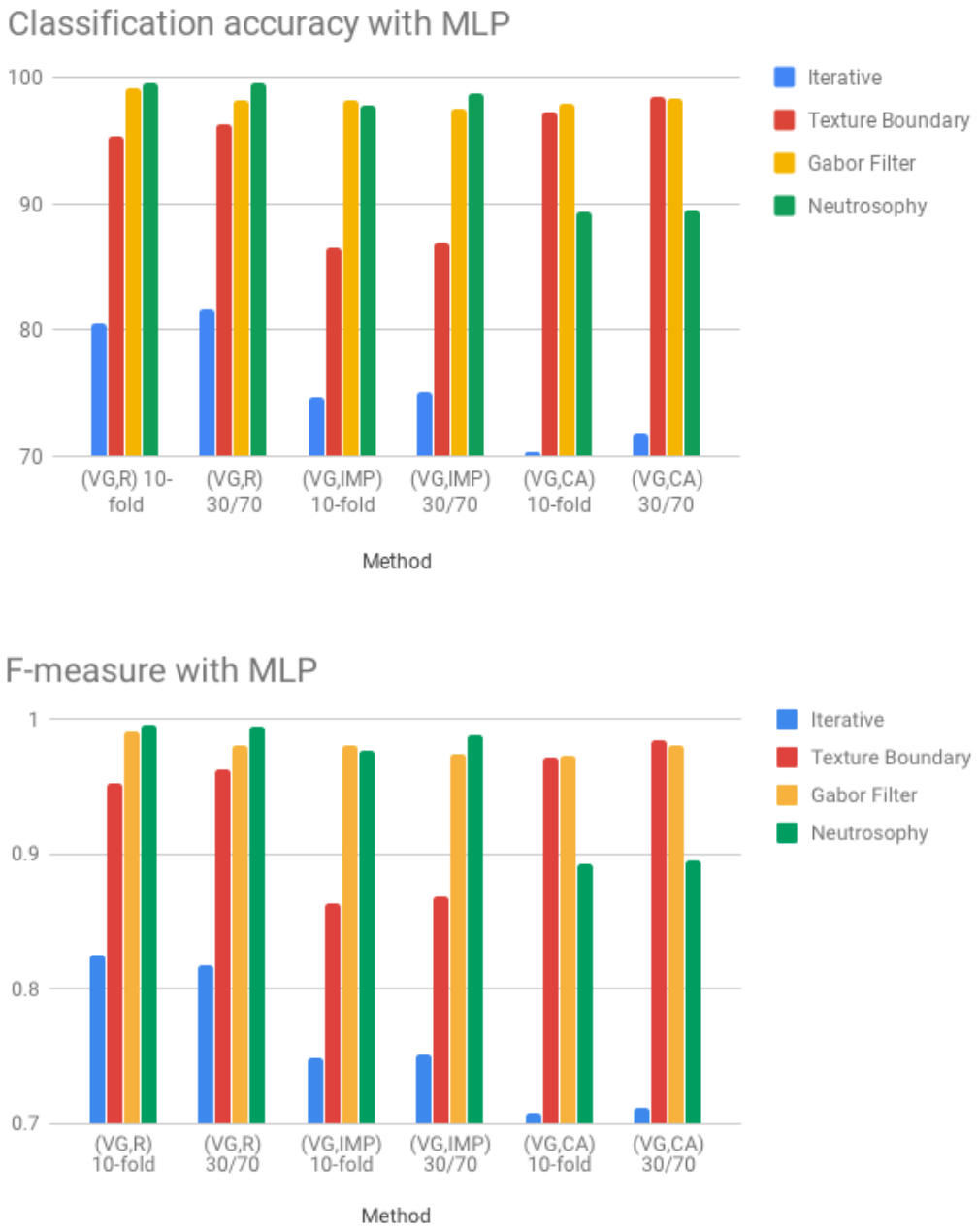

FIGURE 5.15: The performance measurements of the four segmentation methods classified by MLP

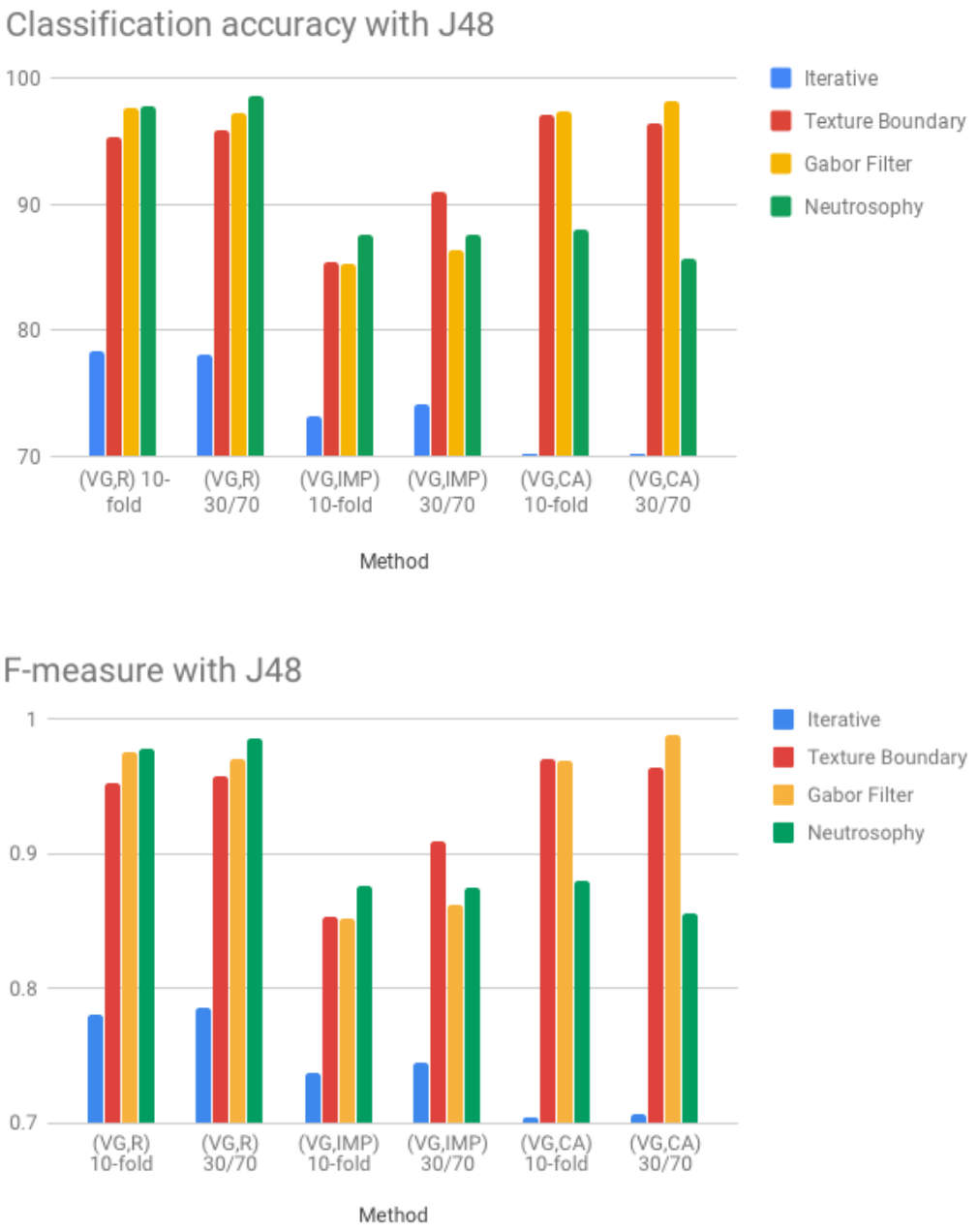

FIGURE 5.16: The performance measurements of the four segmentation methods classified by J48

Chapter 6

Conclusion and Future Works

6.1 Conclusion

To characterize an artistic style is to identify and to extract the elements of artworks and formulate them as a series of distinguishable features. Automatic style characterization can be done in two ways. It can be done by characterizing the global features of the artwork and by identifying the formal elements of the artwork. This thesis automatically characterizes the works of Vincent van Gogh by digitally identifying his paintings' formal elements. We focused on using his brushstrokes as the formal element to be evaluated in characterizing his artistic style. This is because Van Gogh's brushstrokes are a more important component of his style than the other formal elements (McQuillan, 1989).

We developed four methods to segment Van Gogh's brushstrokes: the iterative extraction method, the texture boundary detection method, the Gabor filter based segmentation method, and the Neutrosophy based segmentation method. We focused on the extraction of the visible brushstrokes that are not rendered behind any other brushstrokes.

From the brushstrokes extracted by those methods, we extracted texture and shape features and performed binary classification tests with the works

by three other group of paintings, the works of: Rembrandt, the Impressionists, and Cuno Amiet. Those three groups are chosen based on their degree of similarity to the works of Van Gogh. Rembrandt with his blended brushstrokes and detailed embellishment was the most different, the Impressionists were the predecessors of Van Gogh in creating bold and vivid brushstrokes. Cuno Amiet belong to the same Post-Impressionist artistic movement as Van Gogh and was his contemporary.

Based on the classifications, the most contributing factor for detecting visible brushstroke is the brushstroke's texture. It is shown by our two texture-based segmentation methods, which are texture boundary detection and Gabor-filter segmentation method, that Van Gogh's brushstrokes is more distinguishable from other painters' if they are extracted with respect to their texture. The neutrosophy based segmentation method, generally performs better than any other methods, except for generating features for the classification of Van Gogh and Cuno Amiet. Nevertheless, this method gives the best visual result with the ability to magnify the brushstrokes' inner streaks thus determining their orientations.

6.2 Future Works

As the extension of our research, we would like to incorporate the brushstroke features we have tested in this thesis for the implementation of a stroke based non-photorealistic rendering (NPR). The following ideas can be implemented:

1. The formulation of NPR parameters for representing Van Gogh's brushstroke shapes with respect to his brushstroke's shape features.

2. The formulation of NPR parameters for generating van Gogh's brushstroke texture (impasto) with respect to the Gabor coefficients of his brushstrokes.

3. The construction of a brush model for the stroke-based rendering using coordinated particles.

We also would like to do a further investigation on other formal elements that can be used in describing Van Gogh's artistic style. Some formal elements like light and composition features can be taken into account since Van Gogh's paintings ranging widely from landscape paintings to still life paintings. Furthermore, those additional features can be used to identify his different periods of art.

Bibliography

Agarwal, Siddharth et al. (2015). "Genre and style based painting classification". In: *Applications of Computer Vision (WACV), 2015 IEEE Winter Conference on*. IEEE, pp. 588–594.

Agrawal, Amit and Ramesh Raskar (2007). "Gradient domain manipulation techniques in vision and graphics". In: *ICCV short course*.

Agrawala, Maneesh and Chris Stolte (2001). "Rendering effective route maps: improving usability through generalization". In: *Proceedings of the 28th annual conference on Computer graphics and interactive techniques*. ACM, pp. 241–249.

Ali, SM and RE Burge (1988). "New automatic techniques for smoothing and segmenting SAR images". In: *Signal Processing* 14.4, pp. 335–346.

Barile, Perry, Vic Ciesielski, and Karen Trist (2008). "Non-photorealistic rendering using genetic programming". In: *Simulated Evolution and Learning*. Springer, pp. 299–308.

Berezhnoy, Igor, Eric Postma, and Jaap van den Herik (2007). "Computer analysis of van Gogh's complementary colours". In: *Pattern Recognition Letters* 28.6, pp. 703–709.

Berezhnoy, Igor, Erik Postma, and H.J. Van Den Herik (2009). "Automatic extraction of brushstroke orientation from paintings". In: *Machine Vision and Applications*. Vol. 20, 1, pp. 1–9.

Bhargava, Neeraj et al. (2013). "Decision tree analysis on j48 algorithm for data mining". In: *International Journal of Advanced Research in Computer Science and Software Engineering*. Vol. 3, 6.

Callen, Anthea (1982). *Techniques of the Impressionists*. QED Publishing/Chartwell Books.

Canny, John (1986). "A computational approach to edge detection". In: *Pattern Analysis and Machine Intelligence, IEEE Transactions on* 6, pp. 679–698.

Carrier, David (2003). "In Praise of Connoisseurship". In: *The Journal of aesthetics and art criticism* 61.2, pp. 159–169.

Chang, Chih-Chung and Chih-Jen Lin (2011). "LIBSVM: a library for support vector machines". In: *ACM transactions on intelligent systems and technology (TIST)* 2.3, p. 27.

Charney, Noah (2015). *The Art of Forgery: The Minds, Motives and Methods of Master Forgers*. Phaidon Press Limited.

Chaudhuri, BB and Ujjwal Bhattacharya (2000). "Efficient training and improved performance of multilayer perceptron in pattern classification". In: *Neurocomputing* 34.1-4, pp. 11–27.

Chilvers, Ian and John Glaves-Smith (2009). *A dictionary of modern and contemporary art*. Oxford University Press, USA.

Chu, Wei-Ta and Yi-Ling Wu (2018). "Image Style Classification based on Learnt Deep Correlation Features". In: *IEEE Transactions on Multimedia*.

Clarke, Rachel (2010). "Cataloguing and classification for art and design school libraries: challenges and considerations,'" in: *The handbook of art and design librarianship*, p. 113.

Clausi, David A and M Ed Jernigan (2000). "Designing Gabor filters for optimal texture separability". In: *Pattern Recognition* 33.11, pp. 1835–1849.

Coburn, Erin et al. (2010). "The Cataloging Cultural Objects Experience: Codifying Practice for the Cultural Heritage Community". In: *IFLA Journal* 36.1, pp. 16–29.

Cohen, Patricia, Stephen G West, and Leona S Aiken (2014). *Applied multiple regression/correlation analysis for the behavioral sciences*. Psychology Press.

Cole, Forrester et al. (2009). "How well do line drawings depict shape?" In: *ACM Transactions on Graphics (ToG)*. Vol. 28. 3. ACM, p. 28.

Collomosse, John and Jan Eric Kyprianidis (2011). "Artistic stylization of images and video". In: *Tutorial at Eurographics*.

Collomosse, John P (2008). "Evolutionary search for the artistic rendering of photographs". In: *The Art of Artificial Evolution*. Springer, pp. 39–62.

Collomosse, John P and Peter M Hall (2003). "Cubist style rendering from photographs". In: *Visualization and Computer Graphics, IEEE Transactions on* 9.4, pp. 443–453.

Colton, Simon, Ramon López de Mántaras, and Oliviero Stock (2009). "Computational creativity: Coming of age". In: *AI Magazine* 30.3, pp. 11–11.

Connected Component Labelling. `https://www.cs.auckland.ac.nz/~georgy/research`. Accessed: 2015-01-01.

Connolly, Christine and T. Fleiss (1997). "A study of efficiency and accuracy in the transformation from RGB to CIELAB colour space". In: *IEEE Transactions on Image Processing*. Vol. 6, 7. IEEE, pp. 1046–1048.

Şengür, A. and Y. Guo (2011). "Color texture image segmentation based on neutrosophic set and wavelet transformation". In: *Computer Vision and Image Understanding* 115.8, pp. 1134–1144.

Curtis, Cassidy J et al. (1997). "Computer-generated watercolor". In: *Proceedings of the 24th annual conference on Computer graphics and interactive techniques*. ACM Press/Addison-Wesley Publishing Co., pp. 421–430.

De Silva, Anthony Mihirana and Philip HW Leong (2015). "Grammar Based Feature Generation". In: *Grammar-Based Feature Generation for Time-Series Prediction*. Springer, pp. 35–50.

Deussen, Oliver et al. (2000). "Floating points: A method for computing stipple drawings". In: *Computer Graphics Forum*. Vol. 19. 3. Wiley Online Library, pp. 41–50.

DiPaola, Steve, Caitlin Riebe, and James T Enns (2010). "Rembrandt's textural agency: A shared perspective in visual art and science". In: *Leonardo* 43.2, pp. 145–151.

Douze, Matthijs et al. (2009). "Evaluation of gist descriptors for web-scale image search". In: *Proceedings of the ACM International Conference on Image and Video Retrieval*. ACM, p. 19.

Dutton, Denis (2009). *The art instinct: Beauty, pleasure, & human evolution*. Oxford University Press, USA.

Ester, Martin et al. (1996). "A density-based algorithm for discovering clusters in large spatial databases with noise." In: *Kdd*. Vol. 96. 34, pp. 226–231.

Fisher, R et al. (2003). *Skeletonization/medial axis transform*.

Garnica, Carsten, Frank Boochs, and Marek Twardochlib (2000). "A new approach to edge-preserving smoothing for edge extraction and image segmentation". In: *International Archives of Photogrammetry and Remote Sensing* 33.B3/1; PART 3, pp. 320–325.

Gatys, Leon A, Alexander S Ecker, and Matthias Bethge (2015). "A neural algorithm of artistic style". In: *arXiv preprint arXiv:1508.06576*.

Gerson, Horst, Rembrandt Harmenszoon van Rijn, and Gary Schwartz (1968). *Rembrandt paintings*. Reynal.

Gooch, Amy A et al. (2010). "Viewing progress in non-photorealistic rendering through Heinlein's lens". In: *Proceedings of the 8th International Symposium on Non-Photorealistic Animation and Rendering*. ACM, pp. 165–171.

Gooch, Bruce, Greg Coombe, and Peter Shirley (2002). "Artistic vision: painterly rendering using computer vision techniques". In: *Proceedings of the 2nd international symposium on Non-photorealistic animation and rendering*. ACM, 83–ff.

Gooch, Bruce and Amy Gooch (2001). *Non-photorealistic Rendering*. Natick, MA: AK Peters Ltd.

Graham, Daniel J et al. (2010). "Mapping the similarity space of paintings: image statistics and visual perception". In: *Visual Cognition* 18.4, pp. 559–573.

Grinstein, Georges and Bhavani Thuraisingham (1995). "Data mining and data visualization: Position paper for the second IEEE workshop on database issues for data visualization". In: *Workshop on Database Issues for Data Visualization*. Springer, pp. 54–56.

Guo, Yanhui and Heng-Da Cheng (2009). "New neutrosophic approach to image segmentation". In: *Pattern Recognition* 42.5, pp. 587–595.

Guo, Yanhui and Abdulkadir Şengür (2014). "A novel image segmentation algorithm based on neutrosophic similarity clustering". In: *Applied Soft Computing* 25, pp. 391–398.

Guyon, Isabelle and André Elisseeff (2003). "An introduction to variable and feature selection". In: *Journal of machine learning research* 3.Mar, pp. 1157–1182.

Haeberli, Paul (1990). "Paint by numbers: Abstract image representations". In: *ACM SIGGRAPH Computer Graphics*. Vol. 24. 4. ACM, pp. 207–214.

Hall, Mark A (1998). "Correlation-based feature subset selection for machine learning". In: *Thesis submitted in partial fulfillment of the requirements of the degree of Doctor of Philosophy at the University of Waikato*.

Hammouda, Khaled and Ed Jernigan (2000). "Texture segmentation using gabor filters". In: *Center for Intelligent Machines, McGill University, Québec, Canada*.

Haralick, Robert M, K Shanmugam, Its'Hak Dinstein, et al. (1973). "Textural features for image classification". In: *IEEE Transactions on systems, man, and cybernetics* 3.6, pp. 610–621.

Hausner, Alejo (2001). "Simulating decorative mosaics". In: *Proceedings of the 28th annual conference on Computer graphics and interactive techniques*. ACM, pp. 573–580.

Heard, James (2006). *Paint Like Monet*. Cassell.

Hertzmann, Aaron (1998). "Painterly rendering with curved brush strokes of multiple sizes". In: *Proceedings of the 25th annual conference on Computer graphics and interactive techniques*. ACM, pp. 453–460.

– (2001). "Paint by relaxation". In: *Computer Graphics International 2001. Proceedings*. IEEE, pp. 47–54.

– (2003). "A survey of stroke-based rendering". In: *IEEE Computer Graphics and Applications* 4, pp. 70–81.

– (2010). "Non-photorealistic rendering and the science of art". In: *Proceedings of the 8th International Symposium on Non-Photorealistic Animation and Rendering*. ACM, pp. 147–157.

Huang, Hsueh En, Yew-Soon Ong, and Xianshun Chen (2012). "Autonomous flock brush for non-photorealistic rendering". In: *IEEE Congress On Evolutionary Computation*. IEEE, pp. 378–383.

Huang, Hsueh En et al. (2012). "Interactive GA flock brush for non-photorealistic rendering". In: *Simulated Evolution and Learning*. Springer, pp. 480–490.

Hughes, James M, Daniel J Graham, and Daniel N Rockmore (2010). "Quantification of artistic style through sparse coding analysis in the drawings of Pieter Bruegel the Elder". In: *Proceedings of the National Academy of Sciences* 107.4, pp. 1279–1283.

Icoglu, Oguz, Bilge Gunsel, and Sanem Sariel (2004). "Classification and indexing of paintings based on art movements". In: *EUSIPCO*, pp. 749–752.

Izadi, Ashkan, Vic Ciesielski, and Marsha Berry (2010). "Evolutionary non photo–realistic animations with triangular brushstrokes". In: *AI 2010: Advances in Artificial Intelligence*. Springer, pp. 283–292.

Jain, Anil K, Nalini K Ratha, and Sridhar Lakshmanan (1997). "Object detection using Gabor filters". In: *Pattern recognition* 30.2, pp. 295–309.

Jain, Ramesh, Rangachar Kasturi, and Brian G Schunck (1995). *Machine vision*. Vol. 5. McGraw-Hill New York.

Jansson, Erika (2004). *Brush Painting Algorithms*.

Jiang, Shuqiang et al. (2006). "An effective method to detect and categorize digitized traditional Chinese paintings". In: *Pattern Recognition Letters* 27.7, pp. 734–746.

Jing, Linlin, Kohei Inoue, and Kiichi Urahama (2005). "An NPR technique for pointillistic and mosaic images with impressionist color arrangement". In: *Advances in Visual Computing*. Springer, pp. 1–8.

Johnson, C. Richard et al. (2008). "Image processing for artist identification". In: *IEEE signal processing magazine*. Vol. 25, 4. IEEE, pp. 37–48.

Johnson, M (2008). *Machine Vision*.

Jović, Alan, Karla Brkić, and Nikola Bogunović (2015). "A review of feature selection methods with applications". In: *Information and Communication Technology, Electronics and Microelectronics (MIPRO), 2015 38th International Convention on*. IEEE, pp. 1200–1205.

Jung, C. and J. Scharcanski (2005). "Robust watershed segmentation using wavelets". In: *Image and Vision Computing* 23.7, pp. 661–669.

Kant, Immanuel (2000). *Critique of the Power of Judgment*. Cambridge University Press.

Kashyap, Rangasami L. and K-B Eom (1989). "Texture boundary detection based on the long correlation model". In: *IEEE transactions on pattern analysis and machine intelligence* 11.1, pp. 58–67.

Kaur, Gaganjot and Amit Chhabra (2014). "Improved J48 classification algorithm for the prediction of diabetes". In: *International Journal of Computer Applications* 98.22.

Kennedy, James et al. (2001). *Swarm intelligence*. Morgan Kaufmann.

Kim, Sung Ye et al. (2009). "Stippling by example". In: *Proceedings of the 7th International Symposium on Non-Photorealistic Animation and Rendering*. ACM, pp. 41–50.

Kisilevich, Slava, Florian Mansmann, and Daniel Keim (2010). "P-DBSCAN: a density based clustering algorithm for exploration and analysis of attractive areas using collections of geo-tagged photos". In: *Proceedings of the 1st international conference and exhibition on computing for geospatial research & application*. ACM, p. 38.

Kleinbauer, W Eugene and Thomas P Slavens (1982). *Research guide to the history of Western art*. American Library Association Chicago, IL.

Kodinariya, Trupti M and Prashant R Makwana (2013). "Review on determining number of Cluster in K-Means Clustering". In: *International Journal* 1.6, pp. 90–95.

Kohonen, Teuvo (1998). "The self-organizing map". In: *Neurocomputing* 21.1-3, pp. 1–6.

Korting, Thales Sehn (2006). "C4. 5 algorithm and multivariate decision trees". In: *Image Processing Division, National Institute for Space Research–INPE Sao Jose dos Campos–SP, Brazil*.

Kovesi, Peter D (2000). "MATLAB and Octave functions for computer vision and image processing". In: *Centre for Exploration Targeting, School of Earth and Environment, The University of Western Australia, available from: http://www. csse. uwa. edu. au/ pk/research/matlabfns* 147, p. 230.

Kroner, Sabine and Andreas Lattner (1998). "Authentication of free hand drawings by pattern recognition methods". In: *Pattern Recognition, 1998. Proceedings. Fourteenth International Conference on*. Vol. 1. IEEE, pp. 462–464.

Kyprianidis, Jan Eric et al. (2013). "State of the Art&# x201D;: A Taxonomy of Artistic Stylization Techniques for Images and Video". In: *Visualization and Computer Graphics, IEEE Transactions on* 19.5, pp. 866–885.

Lee, Sang-Geol and Eui-Young Cha (2016). "Style classification and visualization of art painting's genre using self-organizing maps". In: *Human-centric Computing and Information Sciences* 6.1, p. 7.

Lee, Sangwon, Sven C Olsen, and Bruce Gooch (2006). "Interactive 3D fluid jet painting". In: *Proceedings of the 4th international symposium on Non-photorealistic animation and rendering*. ACM, pp. 97–104.

Levinson, Jerrold (2003). *The Oxford handbook of aesthetics*. Oxford University Press.

Li, Jia et al. (2012). "Rhythmic brushstrokes distinguish van Gogh from his contemporaries: findings via automated brushstroke extraction". In: *Pattern Analysis and Machine Intelligence, IEEE Transactions on* 34.6, pp. 1159–1176.

Lin, S (2012). *Non-Photorealistic Rendering*.

Litwinowicz, Peter (1997). "Processing images and video for an impressionist effect". In: *Proceedings of the 24th annual conference on Computer graphics and interactive techniques*. ACM Press/Addison-Wesley Publishing Co., pp. 407–414.

Lombardi, Thomas, Sung-Hyuk Cha, and Charles Tappert (2004). "A graphical user interface for a fine-art painting image retrieval system". In: *ACM SIGMM international workshop on Multimedia information retrieval*. ACM, pp. 107–112.

Lowe, David G. (2004). "Distinctive image features from scale-invariant keypoints". In: *International Journal of Computer Vision*. Vol. 60, 2, pp. 91–110.

McCorduck, Pamela (1991). *Aaron's code: meta-art, artificial intelligence, and the work of Harold Cohen*. Macmillan.

McQuillan, Melissa (1989). *Van Gogh*. Thames and Hudson.

Meer, Peter and Bogdan Georgescu (2001). "Edge detection with embedded confidence". In: *Pattern Analysis and Machine Intelligence, IEEE Transactions on* 23.12, pp. 1351–1365.

Meier, Barbara J (1996). "Painterly rendering for animation". In: *Proceedings of the 23rd annual conference on Computer graphics and interactive techniques*. ACM, pp. 477–484.

Mori, Fumihiko and Terunori Mori (2012). "Region segmentation and object extraction based on virtual edge and global features". In: *Computer Vision-ACCV 2012 Workshops*. Springer, pp. 182–193.

Mould, David (2003). "A stained glass image filter". In: *Proceedings of the 14th Eurographics workshop on Rendering*. Eurographics Association, pp. 20–25.

Nienhaus, Marc and Jürgen Döllner (2004). "Blueprints: illustrating architecture and technical parts using hardware-accelerated non-photorealistic rendering". In: *Proceedings of Graphics Interface 2004*. Canadian Human-Computer Communications Society, pp. 49–56.

Ohta, Yuichi, Takeo Kanade, and Toshiyuki Sakai (1980). "Color information for region segmentation". In: *Computer graphics and image processing* 13.3, pp. 222–241.

Olfati-Saber, Reza (2006). "Flocking for multi-agent dynamic systems: Algorithms and theory". In: *Automatic Control, IEEE Transactions on* 51.3, pp. 401–420.

Oliva, Aude and Antonio Torralba (2001). "Modeling the shape of the scene: A holistic representation of the spatial envelope". In: *International Journal of Computer Vision*. Vol. 42, 3, pp. 145–175.

Ostromoukhov, Victor (1999). "Artistic Halftoning: Between technology and art". In: *Electronic Imaging*. International Society for Optics and Photonics, pp. 489–509.

Otsu, Nobuyuki (1979). "A threshold selection method from gray-level histograms". In: *IEEE transactions on systems, man, and cybernetics* 9.1, pp. 62–66.

Ozden, M. and E Polat (2007). "A color image segmentation approach for content-based image retrieval". In: *Pattern Recognition* 40, pp. 1318–1325.

Pal, Sankar K (1992). "Fuzzy sets in image processing and recognition". In: *Fuzzy Systems, 1992., IEEE International Conference on*. IEEE, pp. 119–126.

Pankhurst, Andy and Lucinda Hawksley (2015). *When Art Really Works*. Phaidon Press Limited.

Pass, Greg, Ramin Zabih, and Justin Miller (1997). "Comparing images using color coherence vectors". In: *Proceedings of the fourth ACM international conference on Multimedia*. ACM, pp. 65–73.

Pearson, Karl (1901). "LIII. On lines and planes of closest fit to systems of points in space". In: *The London, Edinburgh, and Dublin Philosophical Magazine and Journal of Science* 2.11, pp. 559–572.

Pham, Binh (1991). "Expressive brush strokes". In: *CVGIP: Graphical Models and Image Processing* 53.1, pp. 1–6.

Pietikäinen, Matti (2010). "Local binary patterns". In: *Scholarpedia* 5.3, p. 9775.

Pudet, T (1991). "Expressive brush strokes". In: *Elsevier Computer Vision, Graphics, and Image Processing: Graphical Models and Image Processing*. Vol. 53, 1. Elsevier, pp. 1–6.

Putri, Tieta (2012). "Non-photorealistic rendering of pointillist-inspired images by an evolutionary process". MA thesis. RMIT University.

Putri, Tieta and Aniati Murni Arymurthy (2010). "Image feature extraction and recognition of abstractionism and realism style of indonesian paintings". In: *IEEE Advances in Computing, Control and Telecommunication Technologies*. IEEE, pp. 149–152.

Putri, Tieta, Mohamad Ivan Fanany, and Aniati Murni Arymurthy (2011). "Maintaining imbalance highly dependent medical data using dirichlet process data generation". In: *Digital Information Management (ICDIM), 2011 Sixth International Conference on*. IEEE, pp. 18–22.

Putri, Tieta and Ramakrishnan Mukundan (2015). "Iterative brush path extraction algorithm for aiding flock brush simulation of stroke-based painterly rendering". In: *International Conference on Evolutionary and Biologically Inspired Music and Art*. Springer, pp. 152–162.

Putri, Tieta, Ramakrishnan Mukundan, and Kourosh Neshatian (2017). "Artistic Style Characterization of Vincent Van Gogh's Paintings using Extracted Features from Visible Brush Strokes." In: *International Conference on Pattern Recognition Applications and Methods*. Scitepress, pp. 378–385.

Quinlan, J. Ross (1986). "Induction of decision trees". In: *Machine learning* 1.1, pp. 81–106.

Reinhard, Erik et al. (2008). *Color imaging: fundamentals and applications*. CRC Press.

Reynolds, Craig W (1987). "Flocks, herds and schools: A distributed behavioral model". In: *ACM SIGGRAPH computer graphics*. Vol. 21. 4. ACM, pp. 25–34.

Rosseau, Theodore (1968). "The stylistic detection of forgeries". In: *The Metropolitan Museum of Art Bulletin*. Vol. 26, 6. The Metropolitan Museum of Art, pp. 247–252.

Rubin, James Henry (1999). *Impressionism*. Phaidon.

Ruck, Dennis W, Steven K Rogers, and Matthew Kabrisky (1990). "Feature selection using a multilayer perceptron". In: *Journal of Neural Network Computing* 2.2, pp. 40–48.

Russ, John C (2015). *The image processing handbook*. CRC press.

Ryan, Thomas A and Carol B Schwartz (1956). "Speed of perception as a function of mode of representation". In: *The American journal of psychology* 69.1, pp. 60–69.

Salisbury, Michael P et al. (1994). "Interactive pen-and-ink illustration". In: *Proceedings of the 21st annual conference on Computer graphics and interactive techniques*. ACM, pp. 101–108.

Samet, Hanan (1981). "Connected component labeling using quadtrees". In: *Journal of the ACM (JACM)* 28.3, pp. 487–501.

Santella, Anthony and Doug DeCarlo (2004). "Visual interest and NPR: an evaluation and manifesto". In: *Proceedings of the 3rd international symposium on Non-photorealistic animation and rendering*. ACM, pp. 71–150.

Schubert, Erich et al. (2017). "DBSCAN revisited, revisited: why and how you should (still) use DBSCAN". In: *ACM Transactions on Database Systems (TODS)* 42.3, p. 19.

Semet, Yann, Una-May O'Reilly, and Fredo Durand (2004). "An interactive artificial ant approach to non-photorealistic rendering". In: *Genetic and Evolutionary Computation–GECCO 2004*. Springer, pp. 188–200.

Sener, Fadime, Nermin Samet, and Pinar Duygulu Sahin (2012). "Identification of illustrators". In: *European Conference on Computer Vision*. Springer, pp. 589–597.

Seo, SangHyun and HunJoo Lee (2015). "Pixel based stroke generation for painterly effect using maximum homogeneity neighbor filter". In: *Multimedia Tools and Applications* 74.10, pp. 3317–3328.

Seo, SangHyun, YoungSub Park, and Victor Ostromoukhov (2013). "Image recoloring using linear template mapping". In: *Multimedia tools and applications* 64.2, pp. 293–308.

Shannon, Claude Elwood (2001). "A mathematical theory of communication". In: *ACM SIGMOBILE mobile computing and communications review* 5.1, pp. 3–55.

Sheng, Jiachuan and Jianmin Jiang (2013). "Style-based classification of Chinese ink and wash paintings". In: *Optical Engineering* 52.9, p. 093101.

Shiraishi, Michio and Yasushi Yamaguchi (2000). "An algorithm for automatic painterly rendering based on local source image approximation". In: *Proceedings of the 1st international symposium on Non-photorealistic animation and rendering*. ACM, pp. 53–58.

Small, David (1991). "Simulating watercolor by modeling diffusion, pigment, and paper fibers". In: *Electronic Imaging'91, San Jose, CA*. International Society for Optics and Photonics, pp. 140–146.

Smarandache, Florentin (1999). "A Unifying Field in Logics: Neutrosophic Logic." In: *Philosophy*. American Research Press, pp. 1–141.

Sousa, Mario Costa and John W Buchanan (2000). "Observational models of graphite pencil materials". In: *Computer Graphics Forum*. Vol. 19. 1, pp. 27–49.

Strassman, S (1986). "Hairy brushes". In: *1986 Siggraph Conference Proceedings*. Vol. 20. 4, p. 225.

Su, Mu-Chun, Woung-Fei Jean, and Hsiao-Te Chang (1996). "A static hand gesture recognition system using a composite neural network". In: *Fifth IEEE International Conference on Fuzzy Systems*. IEEE, pp. 786–792.

Su, Sara L et al. (2002). "Simulating artistic brushstrokes using interval splines". In: *Proceedings of the 5th IASTED International Conference on Computer Graphics and Imaging*. Citeseer, pp. 85–90.

Sutton, Denys (1987). *Bernard Berenson. The Making of a Legend*. Harvard University Press.

Taylor, Richard P, Adam P Micolich, and David Jonas (1999). "Fractal analysis of Pollock's drip paintings". In: *Nature* 399.6735, p. 422.

Tobias, Orlando José and Rui Seara (2002). "Image segmentation by histogram thresholding using fuzzy sets". In: *IEEE transactions on Image Processing* 11.12, pp. 1457–1465.

Tu, Xiaoyuan and Demetri Terzopoulos (1994). "Artificial fishes: Physics, locomotion, perception, behavior". In: *Proceedings of the 21st annual conference on Computer graphics and interactive techniques*. ACM, pp. 43–50.

Urbanowicz, Ryan J et al. (2017). "Relief-based feature selection: introduction and review". In: *arXiv preprint arXiv:1711.08421*.

Urmson, John O (1989). *The methods of aesthetics*.

Van Uitert, Evert (1981). "Van Gogh's concept of his oeuvre". In: *Simiolus: Netherlands Quarterly for the History of Art*, pp. 223–244.

Vieira, Vilson et al. (2015). "A quantitative approach to painting styles". In: *Physica A: Statistical Mechanics and its Applications*. Vol. 417, pp. 110–129.

Werbos, Paul J (1990). "Backpropagation through time: what it does and how to do it". In: *Proceedings of the IEEE* 78.10, pp. 1550–1560.

Whitted, Turner (1983). "Anti-aliased line drawing using brush extrusion". In: *ACM SIGGRAPH Computer Graphics*. Vol. 17. 3. ACM, pp. 151–156.

Winnemöller, Holger (2013). "NPR in the Wild". In: *Image and Video-Based Artistic Stylisation*. Springer, pp. 353–374.

Witten, Ian H et al. (2016). *Data Mining: Practical machine learning tools and techniques*. Morgan Kaufmann.

Yan, Chengxin, Nong Sang, and Tianxu Zhang (2003). "Local entropy-based transition region extraction and thresholding". In: *Pattern Recognition Letters* 24.16, pp. 2935–2941.

Yang, Chuan-Kai and Hui-Lin Yang (2008). "Realization of Seurat's pointillism via non-photorealistic rendering". In: *The Visual Computer* 24.5, pp. 303–322.

Yang, Yiming and Jan O Pedersen (1997). "A comparative study on feature selection in text categorization". In: *Icml*. Vol. 97, pp. 412–420.

Zang, H. Huang, and C.F. Li (2013). "Stroke style analysis for painterly rendering". In: *Journal of Computer Science and Technology*. Vol. 28, 5. IEEE, pp. 762–775.

Zhu, Ningbo et al. (2009). "A fast 2d otsu thresholding algorithm based on improved histogram". In: *Pattern Recognition, 2009. CCPR 2009. Chinese Conference on*. IEEE, pp. 1–5.